

- Ghosh A, Greenberg ME (1995) Distinct roles for bFGF and NT-3 in the regulation of cortical neurogenesis. *Neuron* 15:89–103.
- Gougeon A, Busso D (2000) Morphologic and functional determinants of primordial and primary follicles in the monkey ovary. *Mol Cell Endocrinol* 163:33–42.
- Hayashi M, Mitsunaga F, Itoh M, Shimizu K, Yamashita A (2000) Development of full-length Trk B-immunoreactive structures in the prefrontal and visual cortices of the macaque monkey. *Anat Embryol (Berl)* 201:139–147.
- Hayashi M, Mitsunaga F, Ohira K, Shimizu K (2001) Changes in BDNF-immunoreactive structures in the hippocampal formation of the aged macaque monkey. *Brain Res* 918:191–196.
- Iwai M, Sato K, Kamada H, Omori N, Nagano I, Shoji M, Abe K (2003) Temporal profile of stem cell division, migration, and differentiation from subventricular zone to olfactory bulb after transient forebrain ischemia in gerbils. *J Cereb Blood Flow Metab* 23:331–341.
- Jin K, Minami M, Lan JQ, Mao XO, Bateur S, Simon RP, Greenberg DA (2001) Neurogenesis in dentate subgranular zone and rostral subventricular zone after focal cerebral ischemia in the rat. *Proc Natl Acad Sci U S A* 98:4710–4715.
- Jin K, Zhu Y, Sun Y, Mao XO, Xie L, Greenberg DA (2002a) Vascular endothelial growth factor (VEGF) stimulates neurogenesis in vitro and in vivo. *Proc Natl Acad Sci U S A* 99:11946–11950.
- Jin K, Mao XO, Sun Y, Xie L, Greenberg DA (2002b) Stem cell factor stimulates neurogenesis in vitro and in vivo. *J Clin Invest* 110:311–319.
- Kawada H, Takizawa S, Takanashi T, Morita Y, Fujita J, Fukuda K, Takagi S, Okano H, Ando K, Hotta T (2006) Administration of hematopoietic cytokines in the subacute phase after cerebral infarction is effective for functional recovery facilitating proliferation of intrinsic neural stem/progenitor cells and transition of bone marrow-derived neural cells. *Circulation* 113:701–710.
- Kim H, Li Q, Hempstead BL, Madri JA (2004) Paracrine and autocrine functions of brain-derived neurotrophic factor (BDNF) and nerve growth factor (NGF) in brain-derived endothelial cells. *J Biol Chem* 279:33538–33546.
- Kobayashi T, Ahlenius H, Thored P, Kobayashi R, Kokaia Z, Lindvall O (2006) Intracerebral infusion of glial cell line-derived neurotrophic factor promotes striatal neurogenesis after stroke in adult rats. *Stroke* 37:2361–2367.
- Kornack DR, Rakic P (2001) The generation, migration, and differentiation of olfactory neurons in the adult primate brain. *Proc Natl Acad Sci U S A* 98:4752–4757.
- Leventhal C, Rafii S, Rafii D, Shahar A, Goldman SA (1999) Endothelial trophic support of neuronal production and recruitment from the adult mammalian subependyma. *Mol Cell Neurosci* 13:450–464.
- Lewis Carl SA, Gillette-Ferguson I, Ferguson DG (1993) An indirect immunofluorescence procedure for staining the same cryosection with two mouse monoclonal primary antibodies. *J Histochem Cytochem* 41:1273–1278.
- Li TS, Hamano K, Nishida M, Hayashi M, Ito H, Mikamo A, Matsuzaki M (2003) CD117⁺ stem cells play a key role in therapeutic angiogenesis induced by bone marrow cell implantation. *Am J Physiol Heart Circ Physiol* 285:H931–H937.
- Lichtenwalner RJ, Parent JM (2006) Adult neurogenesis and the ischemic forebrain. *J Cereb Blood Flow Metab* 26:1–20.
- Lledo PM, Alonso M, Grubb MS (2006) Adult neurogenesis and functional plasticity in neuronal circuits. *Nat Rev Neurosci* 7:179–193.
- Louissaint A Jr, Rao S, Leventhal C, Goldman SA (2002) Coordinated interaction of neurogenesis and angiogenesis in the adult songbird brain. *Neuron* 34:945–960.
- Muzio L, DiBenedetto B, Stoykova A, Boncinelli E, Gruss P, Mallamaci A (2002) Conversion of cerebral cortex into basal ganglia in *Emx2(-/-) Pax6(Sey/Sey)* double-mutant mice. *Nat Neurosci* 5:737–745.
- Okano H (2002) The stem cell biology of the central nervous system. *J Neurosci Res* 69:698–707.
- Otani A, Takagi H, Oh H, Koyama S, Matsumura M, Honda Y (1999) Expressions of angiopoietins and Tie2 in human choroidal neovascular membranes. *Invest Ophthalmol Vis Sci* 40:1912–1920.
- Palmer TD, Willhoite AR, Gage FH (2000) Vascular niche for adult hippocampal neurogenesis. *J Comp Neurol* 425:479–494.
- Palmer TD (2002) Adult neurogenesis and the vascular Nietzsche. *Neuron* 34:856–858.
- Paratcha G, Ibanez CF, Ledda F (2006) GDNF is a chemoattractant factor for neuronal precursor cells in the rostral migratory stream. *Mol Cell Neurosci* 31:505–514.
- Parent JM, Vexler ZS, Gong C, Derugin N, Ferriero DM (2002) Rat forebrain neurogenesis and striatal neuron replacement after focal stroke. *Ann Neurol* 52:802–813.
- Parikh AA, Fan F, Liu WB, Ahmad SA, Stoeltzing O, Reinmuth N, Bielenberg D, Bucana CD, Klagsbrun M, Ellis LM (2004) Neupilin-1 in human colon cancer: expression, regulation, and role in induction of angiogenesis. *Am J Pathol* 164:2139–2151.
- Pencea V, Bingaman KD, Freedman LJ, Luskin MB (2001a) Neurogenesis in the subventricular zone and rostral migratory stream of the neonatal and adult primate forebrain. *Exp Neurol* 172:1–16.
- Pencea V, Bingaman KD, Wiegand SJ, Luskin MB (2001b) Infusion of brain-derived neurotrophic factor into the lateral ventricle of the adult rat leads to new neurons in the parenchyma of the striatum, septum, thalamus, and hypothalamus. *J Neurosci* 21:6706–6717.
- Pincus DW, Keyoung HM, Harrison-Restelli C, Goodman RR, Fraser RA, Edgar M, Sakakibara S, Okano H, Nedergaard M, Goldman SA (1998) Fibroblast growth factor-2/brain-derived neurotrophic factor-associated maturation of new neurons generated from adult human subependymal cells. *Ann Neurol* 43:576–585.
- Pozas E, Ibanez CF (2005) GDNF and GFRalpha1 promote differentiation and tangential migration of cortical GABAergic neurons. *Neuron* 45:701–713.
- Quartu M, Lai ML, Del Fiacco M (1999) Neurotrophin-like immunoreactivity in the human hippocampal formation. *Brain Res Bull* 48:375–382.
- Quartu M, Serra MP, Manca A, Follesa P, Ambu R, Del Fiacco M (2003) High affinity neurotrophin receptors in the human pre-term newborn, infant, and adult cerebellum. *Int J Dev Neurosci* 21:309–320.
- Ruef J, Hu ZY, Yin LY, Wu Y, Hanson SR, Kelly AB, Harker LA, Rao GN, Runge MS, Patterson C (1997) Induction of vascular endothelial growth factor in balloon-injured baboon arteries. A novel role for reactive oxygen species in atherosclerosis. *Circ Res* 81:24–33.
- Sanai N, Tramontin AD, Quinones-Hinojosa A, Barbaro NM, Gupta N, Kunwar S, Lawton MT, McDermott MW, Parsa AT, Manuel-Garcia Verdugo J, Berger MS, Alvarez-Buylla A (2004) Unique astrocyte ribbon in adult human brain contains neural stem cells but lacks chain migration. *Nature* 427:740–744.
- Sandell JH, Baker LS Jr, Davidov T (1998) The distribution of neurotrophin receptor TrkC-like immunoreactive fibers and varicosities in the rhesus monkey brain. *Neuroscience* 86:1181–1194.
- Serra MP, Quartu M, Ambu R, Follesa P, Del Fiacco M (2002) Immunohistochemical localization of GDNF in the human hippocampal formation from prenatal life to adulthood. *Brain Res* 928:138–146.
- Serra MP, Quartu M, Mascia F, Manca A, Boi M, Pisu MG, Lai ML, Del Fiacco M (2005) Ret, GFRalpha-1, GFRalpha-2 and GFRalpha-3 receptors in the human hippocampus and fascia dentata. *Int J Dev Neurosci* 23:425–438.
- Shen Q, Goderie SK, Jin L, Karanth N, Sun Y, Abramova N, Vincent P, Pumiglia K, Temple S (2004) Endothelial cells stimulate self-renewal and expand neurogenesis of neural stem cells. *Science* 304:1338–1340.
- Sun Y, Jin K, Xie L, Childs J, Mao XO, Logvinova A, Greenberg DA (2003) VEGF-induced neuroprotection, neurogenesis, and angiogenesis after focal cerebral ischemia. *J Clin Invest* 111:1843–1851.
- Sun Y, Jin K, Childs JT, Xie L, Mao XO, Greenberg DA (2006) Vascular endothelial growth factor-B (VEGFB) stimulates

- neurogenesis: evidence from knockout mice and growth factor administration. *Dev Biol* 289:329–335.
- Tissot van Patot MC, Bendrick-Pearl J, Beckey VE, Serkova N, Zwerdinger L (2004) Greater vascularity, lowered HIF-1/DNA binding, and elevated GSH as markers of adaptation to in vivo chronic hypoxia. *Am J Physiol Lung Cell Mol Physiol* 287:L525–L532.
- Tonchev AB, Yamashita T, Zhao L, Okano HJ, Okano H (2003) Proliferation of neural and neuronal progenitors after global brain ischemia in young adult macaque monkeys. *Mol Cell Neurosci* 23:292–301.
- Tonchev AB, Yamashita T, Sawamoto K, Okano H (2005) Enhanced proliferation of progenitor cells in the subventricular zone and limited neuronal production in the striatum and neocortex of adult macaque monkeys after global cerebral ischemia. *J Neurosci Res* 81:776–788.
- Uchida T, Nakashima M, Hirota Y, Miyazaki Y, Tsukazaki T, Shindo H (2000) Immunohistochemical localisation of protein tyrosine kinase receptors Tie-1 and Tie-2 in synovial tissue of rheumatoid arthritis: correlation with angiogenesis and synovial proliferation. *Ann Rheum Dis* 59:607–614.
- Walker DG, Beach TG, Xu R, Lile J, Beck KD, McGeer EG, McGeer PL (1998) Expression of the proto-oncogene Ret, a component of the GDNF receptor complex, persists in human substantia nigra neurons in Parkinson's disease. *Brain Res* 79:207–217.
- Wurmser AE, Palmer TD, Gage FH (2004) Neuroscience. Cellular interactions in the stem cell niche. *Science* 304:1253–1255.
- Yamashita T, Kohda Y, Tsuchiya K, Ueno T, Yamashita J, Yoshioka T, Kominami E (1998) Inhibition of ischaemic hippocampal neuronal death in primates with cathepsin B inhibitor CA-074: a novel strategy for neuroprotection based on "calpain-cathepsin hypothesis." *Eur J Neurosci* 10:1723–1733.
- Yamashita T, Tonchev AB, Vachkov IH, Popivanova BK, Seki T, Sawamoto K, Okano H (2004) Vascular adventitia generates neuronal progenitors in the monkey hippocampus after ischemia. *Hippocampus* 14:861–875.
- Zhang RL, Zhang ZG, Zhang L, Chopp M (2001) Proliferation and differentiation of progenitor cells in the cortex and the subventricular zone in the adult rat after focal cerebral ischemia. *Neuroscience* 105:33–41.
- Zhang H, Vutskits L, Pepper MS, Kiss JZ (2003) VEGF is a chemoattractant for FGF-2-stimulated neural progenitors. *J Cell Biol* 163:1375–1384.
- Zhang RL, Zhang ZG, Chopp M (2005) Neurogenesis in the adult ischemic brain: generation, migration, survival, and restorative therapy. *Neuroscientist* 11:408–416.

APPENDIX

Supplementary data

Supplementary data associated with this article can be found, in the online version, at doi: 10.1016/j.neuroscience.2006.10.052.

(Accepted 23 October 2006)
(Available online 22 December 2006)

Inhibition of axonal outgrowth in the tumor environment: Involvement of class 3 semaphorins

Ivan H. Vachkov,^{1,2} Xiaoyong Huang,^{1,3} Yoshihiro Yamada,^{1,3} Anton B. Tonchev,⁴ Tetsumori Yamashima,⁵ Satoru Kato² and Nobuyuki Takakura^{1,3,6}

Departments of ¹Stem Cell Biology, Cancer Research Institute, ²Molecular Neurobiology, Graduate School of Medical Science, Kanazawa University, Kanazawa 920-8640; ³Department of Signal Transduction, Research Institute for Microbial Diseases, Osaka University, 3-1 Yamada-oka, Suita, Osaka 565-0871; ⁴Department of Cell Biology, Division of Forensic Medicine, Varna Medical University, Varna, Bulgaria; ⁵Department of Restorative Neurosurgery, Graduate School of Medical Science, Kanazawa University, Takara-machi 13-1, Kanazawa, 920-8641, Japan

(Received December 21, 2006/Revised April 3, 2007/Accepted April 6, 2007/Online publication May 14, 2007)

That tumors lack innervation is dogma in the field of pathology, but the molecular determinants of this phenomenon remain elusive. We studied the effects of conditioned media from Colon 26 and B16 mouse tumor cell lines on the axonal outgrowth and cellular differentiation of embryonic Institute of Cancer Research (ICR) mouse dorsal root ganglion cells. Tumor-conditioned media suppressed dorsal root ganglion axonal extension but had no effect on neuronal or glial differentiation. We found that the tumor cells expressed most of the class 3 semaphorins – axon guidance molecules. Blocking the activity of class 3 semaphorins with the soluble receptor neuropilin-1 significantly counteracted the tumor-induced inhibition of axonal extension. Together, these results suggest a role for tumor-secreted class 3 semaphorins in selectively inhibiting axonal outgrowth of dorsal root ganglion neurons. (*Cancer Sci* 2007; 98: 1192–1197)

The lack of innervation in tumors is a generally accepted fact,⁽¹⁾ but the molecular determinants of this phenomenon are poorly understood. Furthermore, certain tumors such as esophageal cancer were shown to be innervated by peptidergic nerve fibers and to promote process extension in DRG neurons.⁽²⁾ Notably, sarcomas can secrete NGF, which promotes proliferation and axonal outgrowth of DRG neurons, the observation of which led to the initial discovery of NGF.⁽³⁾ Thus, the effects of tumors on axonal growth are unclear and need further analysis.

Peripheral nerves are known to associate with blood vessels,⁽⁴⁾ reflecting their need for oxygen and nutrients and their control of vasoconstriction and vasodilation.⁽⁵⁾ In mutant embryos containing disorganized nerves, blood vessel branching is altered to follow the nerve,⁽⁶⁾ suggesting that local signals supplied by nerve fibers may provide a template that determines blood vessel patterning. These data indicate a functional relationship between axonal outgrowth and angiogenesis under physiological conditions, and make the question of tumor innervation even more intriguing.

DRG neurons innervate most of the internal organs, thus their processes have the highest potential for interacting with the cells of a tumor growing in the body. We therefore investigated whether molecular cues secreted from tumor cells affect axonal outgrowth and additionally alter the differentiation capacity of immature neural cells in the DRG. Here, we report that supernatant isolated from two tumor cell line cultures inhibited process extension of DRG neurons, and present evidence implicating secreted class 3 semaphorins as mediators of this tumor-induced axonal inhibition.

Materials and Methods

DRG culture. Embryos at embryonic day 12.5 were dissected from pregnant Institute of Cancer Research (ICR) mice (SCL, Shizuoka, Japan). DRG were extracted free of surrounding tissues and

placed one per well in 24-well, poly-L-lysine-coated culture plates (Iwaki, Tokyo, Japan). Colon 26 (C26; mouse colon cancer) and B16 (mouse melanoma) tumor cell lines were cultured in DMEM (Sigma-Aldrich, St Louis, MO, USA) supplemented with 10% FBS (Sigma-Aldrich). Culture supernatants were collected when cells reached approximately 80% confluence. Four culture media were prepared: (i) control medium, DMEM + 10% FBS + 50 ng/mL human recombinant NGF (PeproTech, Rocky Hill, NJ, USA); (ii) tumor-conditioned medium, equal amounts of control medium with 100 ng/mL NGF and tumor cell line supernatant were mixed; (iii) rescue medium, tumor-conditioned medium with 50 µg/mL recombinant fusion protein of the extracellular domain of murine Npn1 with the Fc fragment of human IgG; and (iv) control rescue medium, tumor-conditioned medium with 50 µg/mL recombinant fusion protein of the CD4 glycoprotein with the Fc fragment of human IgG.^(7,8) DRG were incubated in one of the above media for 48 h and then fixed and stained. Culture media were replaced with fresh media after 24 h of incubation.

Immunocytochemistry. The immunohistochemical procedures on culture plates were basically the same as reported previously.⁽⁹⁾ Briefly, DRG on culture plates were fixed in 4% paraformaldehyde in PBS (pH 7.5) for 10 min at RT and rinsed with PBST. Non-specific binding of secondary antibody was blocked with 5% normal goat serum and 1% bovine serum albumin in PBST (blocking serum) for 30 min at RT. Cultures were incubated with mouse anti-β-III tubulin primary antibody (1:200; Covance, Richmond, CA, USA) or rabbit anti-GFAP antibody (1:200; DAKO, Kyoto, Japan) overnight at 4°C in blocking serum, rinsed three times for 10 min at RT with PBST and then incubated with goat antimouse IgG conjugated to Alexa Fluor 488 (1:100; Invitrogen, Carlsbad, CA, USA) in blocking serum for 1 h at RT. Cultures were rinsed again with PBST, and PI was added for 1 min at RT for visualization of nuclei.

RT-PCR. Total RNA was isolated from C26, B16, LLC, cloneM-3 (mouse melanoma) and MM102-TC (mouse mammary gland carcinoma) cells using the Isogen (Wako, Osaka, Japan) isolation kit according to the manufacturer's instructions, and were reverse-transcribed with the SuperScript (Invitrogen) RT-PCR system as reported previously.⁽¹⁰⁾ The class 3 semaphorin Npn1

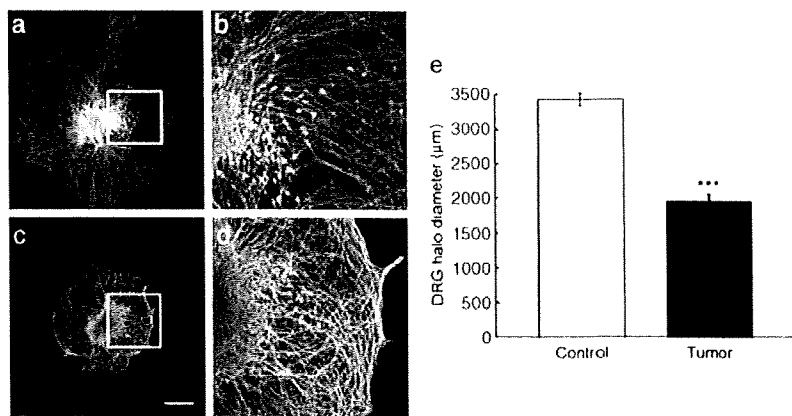
⁵To whom correspondence should be addressed.

E-mail: ntakeku@biken.osaka-u.ac.jp

This work was mainly carried out at Kanazawa University.

Abbreviations: DMEM, Dulbecco's modified Eagle's medium; DRG, dorsal root ganglion; FBS, fetal bovine serum; GFAP, glial fibrillary acidic protein; LLC, Lewis lung carcinoma; NGF, nerve growth factor; Npn, neuropilin; PBS, phosphate-buffered saline; PBST, PBS-Triton X-100; PI, propidium iodide; RT, room temperature; RT-PCR, reverse transcription-polymerase chain reaction; Sema3, semaphorin-3; VEGF, vascular endothelial growth factor.

Fig. 1. Tumor-conditioned medium inhibits dorsal root ganglion (DRG) axonal outgrowth. Confocal images of DRG primary cultures exposed to (a,b) control medium or (c,d) colon 26 tumor-conditioned medium. Cultured cells were stained with anti- β -III tubulin antibody. (b,d) High-power views of areas indicated by boxes in (a) and (c), respectively. Scale bar = 500 μ m. (e) Statistical evaluation of the DRG halo diameter. Data show mean \pm SEM from five random fields. * $P < 0.001$ versus control. Shown are representative data from one of three independent experiments.



and Npn2, and β -actin gene sequences were amplified using ExTaq (TaKaRa, Tokyo, Japan) DNA polymerase with: *Sema3A* forward, 5'-CGGGACTTCGCTATCTTCAG-3' and reverse, 5'-GGGACCATCTCTGTGAGCAT-3'; *Sema3B* forward, 5'-AACCC-ATGCTTCAACTGGAC-3' and reverse, 5'-CTGGAGGTGGAG-AAGACAGC-3'; *Sema3C* forward, 5'-TGGCCACTCTTGC-TCTAGGT-3' and reverse, 5'-GCCTTCAGCTTGCCATAGTC-3'; *Sema3D* forward, 5'-AGCACCGACCTTCAAGAGAA-3' and reverse, 5'-GTGCATATCTGGAGCAAGCA-3'; *Sema3E* forward, 5'-TTGGACAGCAATTTGTTGGA-3' and reverse, 5'-AGCCA-ATCAGCTGCAAGAAT-3'; *Sema-3F* forward, 5'-TGCTTGTC-ACTGCCTTCATC-3' and reverse, 5'-TACAGGTGTGTTCCGGT-TCCA-3'; *Sema3G* forward, 5'-TCTTTGGCACAGACACAAC-3' and reverse, 5'-CCTGCACCATACACGTTAC-3'; *Npn1* forward, 5'-CTCCCGCTGAACCTACCCTGAAAAT-3' and reverse, 5'-CCACTTGGAGCCATTTCATTGGTGTA-3'; *Npn2* forward, 5'-TGAATCTCCAGGGTTCCAG-3' and reverse, 5'-GTCCACCTCCCATCAGAGAA-3'; and β -actin forward, 5'-CCTAAGGCCAACCGTAAAAG-3' and reverse, 5'-TCTTC-ATGGTGCTAGGAGCAG-3' primer pairs. The PCR products were fractionated by electrophoresis and the positive bands were visualized in a FAS III (Toyobo, Osaka, Japan) ultraviolet transilluminator.

Western blotting. C26 and B16 cells were trypsinized and collected. Procedures for the preparation of cell lysates and western blotting were basically the same as those reported previously.⁽¹¹⁾ Briefly, total protein was extracted using Nonidet (N)P-40 Tris buffer with proteinase inhibitor cocktail added. Proteins were fractionated by sodium dodecylsulfate-polyacrylamide gel electrophoresis and transferred to a membrane. The membrane was incubated for 30 min at RT with a generic protein to cover any remaining sticky places. Primary antibodies against mouse *Sema3A* (1:1000; Abcam, Cambridge, UK), *Sema3C* (1:1000; R&D Systems, Minneapolis, MN, USA) or glyceraldehyde-3-phosphate dehydrogenase (1:1000; Chemicon, Temecula, CA, USA) were added for 1 h at RT followed by horseradish peroxidase (HRP)-conjugated goat antimouse IgG (1:1000; DAKO). The positive bands were visualized by ECL detection reagents (Amersham Biosciences, Piscataway, NJ, USA) in a LAS-3000 imaging system (Fujifilm, Tokyo, Japan).

Image analysis. Single and double labeling were visualized by confocal laser scanning microscopy (LSM 510; Carl Zeiss, Göttingen, Germany). Alexa Fluor 488 was assigned to the green channel and PI to the red channel. For single-labeling experiments, an average of 16 z-axis scans was used to generate the final images. In double-labeling experiments, each fluorochrome was scanned separately and sequentially to minimize the probability of signal transfer among channels. Measurements of DRG halo diameter were carried out using Zeiss LSM software version 3.2 on six samples from each experimental group.

Within each experimental group, at least 100 PI-positive cells were investigated for costaining with β -III tubulin or GFAP. Diameters and percentages of positive cells were averaged to obtain a mean density for each marker per experimental group.

Statistical analysis. Diameters of DRG halos were compared using Student's paired *t*-test. Percentages of cells expressing β -III tubulin or GFAP were compared using non-parametric tests (Mann-Whitney *U*-test and Kruskal-Wallis test). Data are expressed as mean \pm SEM. Differences were considered significant when $P < 0.05$.

Results

Tumor-conditioned medium inhibited DRG axonal outgrowth. DRG cells cultured under normal conditions (control medium) grew steadily, and within 48 h of culturing extended radial processes in all directions (Fig. 1a,b), in agreement with previous studies using similar culture media (DMEM supplemented with NGF).^(12,13) The removal of NGF from the culture medium resulted in extensive cell death (data not shown); therefore, all culture media were supplemented with NGF. In contrast, the DRG cells cultured with C26 (Fig. 1c) or B16 (Suppl. Fig. 1) tumor-conditioned medium showed limited axonal outgrowth and their axons lacked the straightness of control axons (Fig. 1d). Quantitative measurement of DRG halo diameters revealed that DRG cells grown in tumor-conditioned medium had significantly smaller halos than those grown in control medium (Fig. 1e).

Tumor-conditioned medium did not alter DRG cellular differentiation. Tumor-conditioned medium affected axonal outgrowth; however, tumor-conditioned medium may also be involved in other cellular processes such as differentiation of DRG cells. Therefore, we stained DRG cells cultured in control or tumor-conditioned media with antibodies against the neuronal marker β -III tubulin or the astrocyte marker GFAP; the nuclei of all cells were counterstained with the DNA-binding dye PI (Fig. 2a-l). We then quantitatively evaluated the percentages of β -III tubulin- or GFAP-positive cells among the total population of PI-stained cells under high magnification (Fig. 2m,n). We evaluated β -III tubulin-positive neuronal cells adjacent to the center of the DRG halo because the density of neuronal cells in the center was too high to clearly distinguish individual cells, but we evaluated GFAP-labeled astrocyte lineage cells in the periphery of the DRG halo where the incidence of astrocytes was high. The β -III tubulin-positive cells in both control (Fig. 2a-c) and tumor-conditioned media (Fig. 2d-f) had similar appearance, and quantitative analysis of the percentage of β -III tubulin-positive cells revealed that there was no significant difference between the control and tumor conditions (Fig. 2m). Likewise, the GFAP-positive cells in both control (Fig. 2g-i)

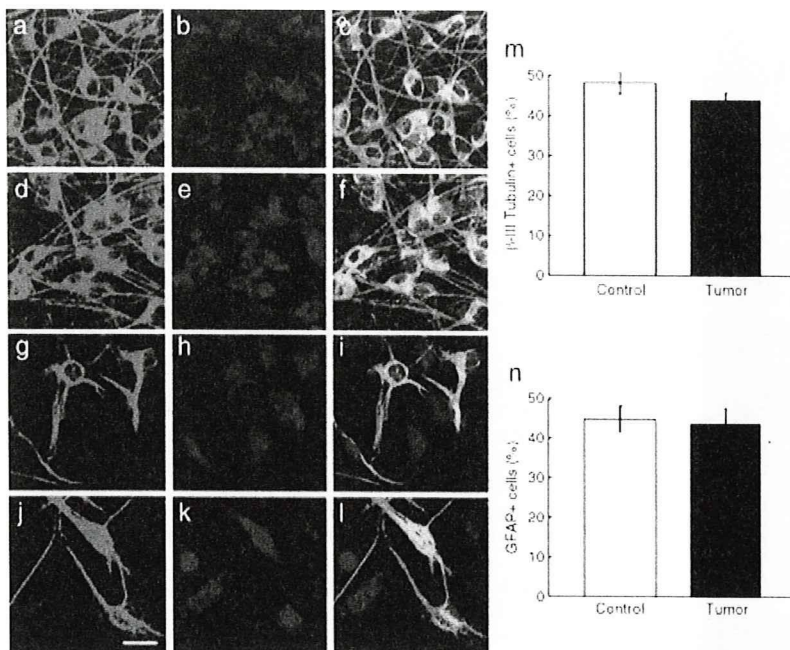


Fig. 2. Tumor-conditioned medium does not affect neuronal or glial differentiation of dorsal root ganglion (DRG) cells. Neuronal or glial cell development of DRG cells in primary cultures exposed to (a–c, g–i) control medium or (d–f, j–l) colon 26 tumor-conditioned medium was analyzed by staining for (a,d) the neuronal marker β -III tubulin or (g,j) the astrocyte marker glial fibrillary acidic protein (GFAP). Cells in (a,d,g,j) were counterstained with propidium iodide (PI) (b,e,h,k, respectively). The images in (c,f,i,l) are merged images of (a,b), (d,e), (g,h) and (j,k). Scale bar = 20 μ m. (m,n) Percentage of β -III tubulin-positive neuronal cells (m) or GFAP-positive glial cells (n) among the total PI-positive cells in DRG primary cultures exposed to control or colon 26 tumor-conditioned medium. Data are mean \pm SEM from five random fields. Shown are representative data from one of three independent experiments.

and tumor-conditioned media (Fig. 2j–l) had similar appearances, and there were no significant differences in the percentage of astroglial cells in the two conditions (Fig. 2n). Together, these results indicate that suppression of DRG axonal outgrowth in tumor-conditioned medium did not result from an altered differentiation of the DRG cells into neuronal and astrocyte lineages.

Effects of tumor-conditioned medium on DRG were dependent on class 3 semaphorins. Based on the above results, we searched for molecular cues in the tumor-conditioned medium that potentially inhibit axonal outgrowth from DRG cells. Due to its well-known growth cone repulsive effects,^(14–17) and because it is the only secreted class of the semaphorin family of proteins in vertebrates,⁽¹⁸⁾ we examined class 3 semaphorin expression in C26 and B16 tumor cells. We found that both C26 and B16 cells expressed Sema3A, Sema3B, Sema3C, Sema3D, Sema3E and Sema3F mRNA (Fig. 3a). Moreover, we found that other cancer cell lines, such as LLC, cloneM-3 (mouse melanoma) and MM102-TC (mouse mammary gland carcinoma) also express several class 3 semaphorins. Interestingly, the tumor cells we observed expressed more or less either Npn1 or Npn2, receptors for class 3 semaphorins. Further, western blotting of tumor cell revealed the presence of Sema3A and Sema3C proteins from both Colon26 and B16 cells (Fig. 3b).

As class 3 semaphorins are soluble ligands for Npn1, we tried to inactivate the function of Sema3 in the cultures. For this purpose we generated a recombinant fusion protein (Npn1-Fc) of the extracellular domain of murine Npn1 and the Fc fragment of human IgG.^(7,8) In the presence of Npn1-Fc (50 μ g/mL), DRG cells cultured in C26 tumor-conditioned medium (Fig. 4e,f) appeared to show more extensive axonal outgrowth than those cultured in C26 tumor-conditioned medium containing the CD4-Fc control protein (Fig. 4c,d), but less than those cultured in control medium (Fig. 4a,b). Morphometric analyses confirmed this impression, as the DRG halo diameters in C26 tumor-conditioned media with Npn1-Fc were significantly larger than those in C26 tumor-conditioned media alone, but still significantly smaller than that with control medium (Fig. 4g). A lower concentration of Npn1-Fc (10 μ g/mL) produced results that were not significantly

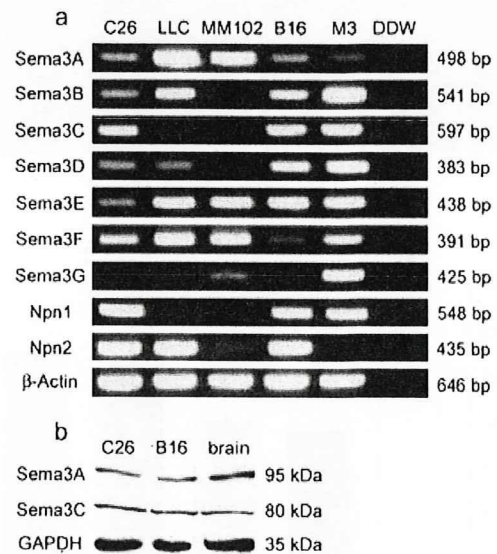


Fig. 3. Tumor cell lines express class 3 semaphorins. (a) Reverse transcription-polymerase chain reaction analysis of mRNA extracted from colon 26 (C26) cells, B16 cells, lewis lung carcinoma (LLC), cloneM-3 (mouse melanoma) and MM102-TC (mouse mammary gland carcinoma). Distilled water was used as a negative control. Non-reverse transcribed RNA did not generate any polymerase chain reaction product. β -Actin was used as an internal loading control. (b) Western blotting of C26 and B16 cells. Glyceraldehyde-3-phosphate was used as an internal control.

different from those in the C26 tumor-conditioned medium, and an excess of the Npn1-Fc (250 μ g/mL) did not add to its rescue effects for axonal outgrowth (Fig. 4g). As observed in the effect of Npn1-Fc for C26 tumor-conditioned media, in the presence of Npn1-Fc DRG cells cultured in B16 tumor-conditioned

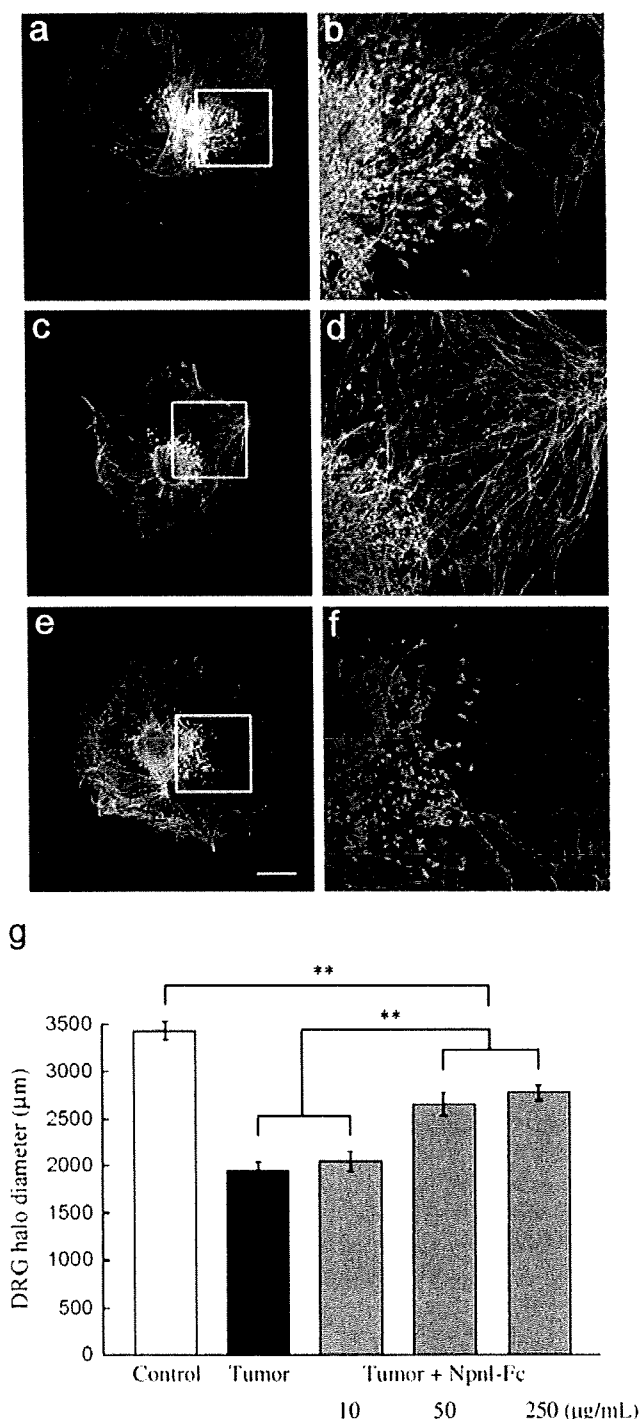


Fig. 4. Inactivation of class 3 semaphorins rescues dorsal root ganglion (DRG) axonal outgrowth. Confocal images of (a,b) DRG primary cultures grown in control medium, (c,d) colon 26 tumor-conditioned medium with CD4-Fc control protein, or (e,f) colon 26 tumor-conditioned medium with 50 µg/mL neuropilin-1-Fc protein. Cultured cells were stained with anti-β-III tubulin antibody. (b,d,f) High-power views of the areas indicated by boxes in (a,c,e). Scale bar = 500 µm. (g) Quantitative evaluation of the DRG halo diameter. Control, control medium; tumor, colon 26 tumor-conditioned medium. Data show mean ± SEM from five random fields. Shown are representative data from one of three independent experiments. * $P < 0.01$.

medium appeared to exhibit more extensive axonal outgrowth than those cultured in B16 tumor-conditioned medium containing the CD4-Fc control protein (Suppl. Fig. 1).

Discussion

The nervous and vascular systems share several anatomical parallels and both systems utilize a complex branching network of neuronal cells or blood vessels to control all regions of the body. From the anatomical and juxtapositional similarities of the nervous and vascular systems, it has been suggested that axons might guide blood vessels, and vice versa. Indeed, VEGF (or VEGF-A) from neuronal cells guides blood vessels,⁽⁶⁾ and signals from vessels, such as artemin and neurotrophin 3, attract axons to track alongside the vessel.^(19,20) In this manner, the neuronal and vascular systems are coordinately well organized in normal tissues; however, in tumor tissues, with a few exceptions, little innervation is observed. In adulthood, regenerated tissue responding to tissue damage is reinnervated along with angiogenesis. Although angiogenesis is commonly observed in the tumor environment and regenerated normal tissue area, why innervation does not occur in the tumor environment has not been elucidated at the molecular level. In the present study, we found one candidate that inhibits innervation in tumors, class 3 semaphorins, molecules well known to induce repulsion of axons.^(15–18)

A series of genetic and biochemical screens identified proteins acting in an instructive manner to actively attract or repel axons, and four types of molecules relating to axon guidance have been isolated, including members of the semaphorin, ephrin, netrin and slit families.⁽²¹⁾ In the present study, it was clear that soluble factors inhibited axon outgrowth because we used the culture supernatant of tumor cells to examine outgrowth in cultured DRG cells. Therefore, among the four kinds of axon guidance molecules described above, we excluded the ephrin family because they are membrane proteins.⁽²²⁾ Moreover, two of the other families of molecules, netrins and slits, function as both attractive and repulsive cues to axons depending on their concentrations in the foci, and originally attract commissural axons to the midline of the brain.⁽²¹⁾ Conversely, several papers have reported semaphorin expression associated with tumor angiogenesis in the tumor environment.^(23,24) Based on this evidence, we examined semaphorin expression in tumor cells.

Semaphorins are a large family of signaling proteins, both secreted and membrane bound. They are divided into eight classes. Among these, class 3 semaphorins (Sema3A–G) are the only secreted forms in vertebrates. Moreover, all class 3 semaphorins were shown to be chemorepulsive for many class of axons, and so far Sema3A, Sema3C, Sema3D and Sema3E were found to bind Npn1 with high affinity.⁽²³⁾ Among the class 3 semaphorins, Sema3A has been most intensively studied in relation to axon guidance.^(15–18) Sema3A shows repulsive activity toward a variety of neuronal types, including motor, sensory, olfactory and hippocampal neurons.^(25–30) Npn1 and Npn2 were the first receptors identified for Sema3A.^(31,32) The transmembrane protein Npn1 forms a homodimer receptor complex for Sema3A. Mice lacking Npn1 have a similar phenotype to those lacking Sema3A, namely, marked defasciculation of nerve bundles and aberrant projections of sensory nerves.^(33,34) Although Npn1 itself does not contain a kinase domain or binding site of the adaptor protein for signal transduction in the cytoplasmic domain, together with plexins it forms a functional receptor complex to induce signals into cells.^(13,35) In this way, Sema3A was studied extensively and is suggested to induce strong chemorepulsion for almost all axons. Therefore, we first tried to knockdown the *Sema3A* gene in C26 and B16 tumor cells, with Sema3A-depleted C26 or B16 tumor-conditioned media being used in DRG culture. However, merely depletion of Sema3A from tumor-conditioned

media did not alter tumor-conditioned media-mediated inhibition of axon outgrowth from DRG (data not shown). Consistent with the result of the *Sema3A* knockdown, our present data showed that almost all class 3 semaphorins were produced from tumor cells, and that soluble Npn1 protein rescued axon outgrowth resulting from tumor-conditioned media. Therefore, we confirm that class 3 semaphorins derived from tumor cells are involved in the inhibition of axon outgrowth. However, soluble Npn1 did not completely rescue the extension of axons to the control level. It is possible that other secreted molecules, including some members of class 3 semaphorins, bind to Npn2 alone. Moreover, in the present study, we focused on soluble proteins for axon extension; however, axon outgrowth is controlled not only by secreted factors but also by cell-to-cell contact-dependent mechanisms. Therefore, molecules expressed on cells within the tumor, such as endothelial cells and tumor fibroblasts, as well as tumor cells, might affect axon guidance in a cell-to-cell contact manner.

References

- Willis RA. *The Spread of Tumors in the Human Body*, 3rd edn. London: Butterworths, 1973.
- Lu SH, Zhou Y, Que HP, Liu SJ. Peptidergic innervation of human esophageal and cardiac carcinoma. *World J Gastroenterol* 2003; **9**: 399–403.
- Levi-Montalcini R. The nerve growth factor 35 years later. *Science* 1987; **237**: 1154–62.
- Martin P, Lewis J. Origins of the neurovascular bundle: interactions between developing nerves and blood vessels in embryonic chick skin. *Int J Dev Biol* 1989; **33**: 379–87.
- Burnstock G, Ralevic V. New insights into the local regulation of blood flow by perivascular nerves and endothelium. *Br J Plast Surg* 1994; **47**: 527–43.
- Mukoyama Y, Shin D, Britsch S, Taniguchi M, Anderson DJ. Sensory nerves determine the pattern of arterial differentiation and blood vessel branching in the skin. *Cell* 2002; **109**: 693–705.
- Yamada Y, Takakura N, Yasue H, Ogawa H, Fujisawa H, Suda T. Exogenous clustered Neuropilin-1 enhances vasculogenesis and angiogenesis. *Blood* 2001; **97**: 1671–8.
- Yamada Y, Oike Y, Ogawa H *et al.* Neuropilin-1 on hematopoietic cells as a source of vascular development. *Blood* 2003; **101**: 1801–9.
- Takakura N, Watanabe T, Suenobu S *et al.* A role for hematopoietic stem cells in promoting angiogenesis. *Cell* 2000; **102**: 199–209.
- Ueno M, Itoh M, Kong L, Sugihara K, Asano M, Takakura N. PSF1 is essential for early embryogenesis in mice. *Mol Cell Biol* 2005; **25**: 10 528–32.
- Kong L, Ueno M, Itoh M, Yoshioka K, Takakura N. Identification and characterization of mouse PSF1-binding protein, SLD5. *Biochem Biophys Res Commun* 2006; **339**: 1204–7.
- Thippeswamy T, McKay JS, Quinn J, Morris R. Either nitric oxide or nerve growth factor is required for dorsal root ganglion neurons to survive during embryonic and neonatal development. *Dev Brain Res* 2005; **154**: 153–64.
- Toyofuku T, Yoshida J, Sugimoto T *et al.* FARP2 triggers signals for Sema3A-mediated axonal repulsion. *Nat Neurosci* 2005; **8**: 1712–19.
- Tessier-Lavigne M, Goodman TS. The molecular biology of axon guidance. *Science* 1996; **274**: 1123–33.
- Tanelian DL, Barry MA, Johnston SA, Le T, Smith GM. Semaphorin III can repulse and inhibit adult sensory afferents *in vivo*. *Nat Med* 1997; **3**: 1398–401.
- Dickson BJ. Molecular mechanisms of axon guidance. *Science* 2002; **298**: 1959–64.
- Guan KL, Rao Y. Signalling mechanisms mediating neuronal responses to guidance cues. *Nat Rev Neurosci* 2003; **4**: 941–56.
- Semaphorin Nomenclature Committee. Unified nomenclature for the semaphorins/collapsins. *Cell* 1999; **97**: 551–5.
- Honma Y, Araki T, Gianino S *et al.* Artemin is a vascular-derived neurotrophic factor for developing sympathetic neurons. *Neuron* 2002; **35**: 267–82.
- Kuruvilla R, Zweifel LS, Glebova NO *et al.* A neurotrophin signaling cascade coordinates sympathetic neuron development through differential control of TrkA trafficking and retrograde signaling. *Cell* 2004; **118**: 243–55.
- Chilton JK. Molecular mechanisms of axon guidance. *Dev Biol* 2006; **292**: 13–24.
- Eichmann A, Makinen T, Alitalo K. Neural guidance molecules regulate vascular remodeling and vessel navigation. *Genes Dev* 2005; **19**: 1013–21.
- Chedotal A, Kerjan G, Moreau-Fauvarque C. The brain within the tumor: new roles for axon guidance molecules in cancers. *Cell Death Differ* 2005; **12**: 1044–56.
- Bielenberg DR, Pettaway CA, Takashima S, Klagsbrun M. Neuropilins in neoplasms: expression, regulation, function. *Exp Cell Res* 2006; **312**: 584–93.
- Chedotal A, Del Rio JA, Ruiz M *et al.* Semaphorins III and IV repel hippocampal axons via two distinct receptors. *Development* 1998; **125**: 4313–23.
- Kobayashi H, Koppel AM, Luo Y, Raper JA. A role for collapsin-1 in olfactory and cranial sensory axon guidance. *J Neurosci* 1997; **17**: 8339–52.
- Koppel AM, Feiner L, Kobayashi H, Raper JA. A 70 amino acid region within the semaphorin domain activates specific cellular response of semaphorin family members. *Neuron* 1997; **19**: 531–7.
- Luo Y, Raible D, Raper JA. Collapsin: a protein in brain that induces the collapse and paralysis of neuronal growth cones. *Cell* 1993; **75**: 217–27.
- Luo Y, Shepherd I, Li J, Renzi MJ, Chang S, Raper JA. A family of molecules related to collapsin in the embryonic chick nervous system. *Neuron* 1995; **14**: 1131–40.
- Messersmith EK, Leonardo ED, Shatz CJ, Tessier-Lavigne M, Goodman CS, Kolodkin AL. Semaphorin III can function as a selective chemorepellent to pattern sensory projections in the spinal cord. *Neuron* 1995; **14**: 949–59.
- He Z, Tessier-Lavigne M. Neuropilin is a receptor for the axonal chemorepellent Semaphorin III. *Cell* 1997; **90**: 739–51.
- Kolodkin AL, Levengood DV, Rowe EG, Tai YT, Giger RJ, Ginty DD. Neuropilin is a semaphorin III receptor. *Cell* 1997; **90**: 753–62.
- Kitsukawa T, Shimizu M, Sanbo M *et al.* Neuropilin-semaphorin III/D-mediated chemorepulsive signals play a crucial role in peripheral nerve projection in mice. *Neuron* 1997; **19**: 995–1005.
- Taniguchi M, Yuasa S, Fujisawa H *et al.* Disruption of semaphorin III/D gene causes severe abnormality in peripheral nerve projection. *Neuron* 1997; **19**: 519–30.
- Pasterkamp RJ, Kolodkin AL. Semaphorin junction: making tracks toward neural connectivity. *Curr Opin Neurobiol* 2003; **13**: 79–89.
- Jain RK. Normalization of tumor vasculature: an emerging concept in antiangiogenic therapy. *Science* 2005; **307**: 58–62.

Supplementary Material

The following supplementary material is available for this article:

Fig. S1. B16 tumor-conditioned medium inhibits dorsal root ganglion (DRG) axonal outgrowth, and inactivation of class 3 semaphorins rescues DRG axonal outgrowth. Immunofluorescence images of DRG primary cultures exposed to (a) control medium, (b) B16 tumor-conditioned medium, or (c) B16 tumor-conditioned medium with 50 µg/mL neuropilin-1-Fc protein. Cultured cells

were stained with anti- β -III tubulin antibody. Shown are representative data from one of three independent experiments. Scale bar = 500 μ m. (d) Statistical evaluation of the DRG halo diameter. Data show mean \pm SEM from five random fields. * $P < 0.01$.

This material is available as part of the online article from:

<http://www.blackwell-synergy.com/doi/abs/10.1111/j.1349-7006.2007.00508.x>

<<http://www.blackwell-synergy.com/doi/abs/10.1111/j.1349-7006.2007.00508.x>>

(This link will take you to the article abstract).

Please note: Blackwell Publishing are not responsible for the content or functionality of any supplementary materials supplied by the authors. Any queries (other than missing material) should be directed to the corresponding author for the article.

Prox1 Induces Lymphatic Endothelial Differentiation via Integrin $\alpha 9$ and Other Signaling Cascades

Koichi Mishima,^{*,†} Tetsuro Watabe,^{*} Akira Saito,^{*} Yasuhiro Yoshimatsu,^{*} Natsuko Imaizumi,^{*} Shinji Masui,[‡] Masanori Hirashima,[§] Tohru Morisada,[§] Yuichi Oike,[§] Makoto Araie,[†] Hitoshi Niwa,[‡] Hajime Kubo,^{||} Toshio Suda,[§] and Kohei Miyazono^{*,||}

Departments of ^{*}Molecular Pathology and [†]Ophthalmology, Graduate School of Medicine, University of Tokyo, Tokyo 113-0033, Japan; [‡]Laboratory for Pluripotent Cell Studies, RIKEN Center for Developmental Biology, Kobe 650-0047, Japan; [§]Department of Cell Differentiation, The Sakaguchi Laboratory, School of Medicine, Keio University, Shinanomachi, Tokyo 160-8582, Japan; ^{||}Molecular and Cancer Research Unit, Horizontal Medical Research Organization (HMRO), Graduate School of Medicine, Kawaramachi, Kyoto University, Kyoto 606-8501, Japan; and ^{||}Department of Biochemistry, The Cancer Institute of the Japanese Foundation for Cancer Research, Ariake, Tokyo 135-8550, Japan

Submitted September 5, 2006; Revised January 2, 2007; Accepted January 31, 2007
Monitoring Editor: Ben Margolis

During embryonic lymphatic development, a homeobox transcription factor Prox1 plays important roles in sprouting and migration of a subpopulation of blood vessel endothelial cells (BECs) toward VEGF-C-expressing cells. However, effects of Prox1 on endothelial cellular behavior remain to be elucidated. Here, we show that Prox1, via induction of integrin $\alpha 9$ expression, inhibits sheet formation and stimulates motility of endothelial cells. Prox1-expressing BECs preferentially migrated toward VEGF-C via up-regulation of the expression of integrin $\alpha 9$ and VEGF receptor 3 (VEGFR3). In mouse embryos, expression of VEGFR3 and integrin $\alpha 9$ is increased in Prox1-expressing lymphatic endothelial cells (LECs) compared with BECs. Knockdown of Prox1 expression in human LECs led to decrease in the expression of integrin $\alpha 9$ and VEGFR3, resulting in the decreased chemotaxis toward VEGF-C. These findings suggest that Prox1 plays important roles in conferring and maintaining the characteristics of LECs by modulating multiple signaling cascades and that integrin $\alpha 9$ may function as a key regulator of lymphangiogenesis acting downstream of Prox1.

INTRODUCTION


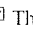
The major roles of the lymphatic vessels are to drain interstitial fluid that leaks out from the blood capillaries and to return it to the blood vessels. In addition, the lymphatic system performs an immune function by transporting immune cells that patrol the tissues to the lymphoid organs (Witte *et al.*, 2001). Insufficiency or obstruction of the lymphatics results in lymphedema, characterized by disabling swelling of the affected tissues. In addition, in many types of cancer, the lymphatic vessels provide a major pathway for tumor metastasis, and regional lymph node metastasis has been shown to be correlated with cancer progression (Karpanen and Alitalo, 2001).

Despite the importance of lymphatic vessels in both normal and pathological conditions, progress in the study of

lymphangiogenesis had been hampered by the lack of specific markers. Recent studies have revealed the various transcriptional and signaling components that play important roles in lymphatic development. Embryonic lymphatic endothelial cells (LECs) arise by sprouting from the jugular veins and migrate to form primary lymphatic plexus (Oliver, 2004). In E10 mouse embryos, the *prospero*-related transcription factor Prox1 is expressed in a subset of ECs of the cardinal vein, from which they sprout to form primary lymph sacs (Wigle and Oliver, 1999; Wigle *et al.*, 2002). In *Prox1*-null mice, sprouting of LECs from the veins appears unaffected at embryonic day (E)10.5, but their migration is arrested at around E11.5–E12.0, leading to a complete absence of the lymphatic vasculature. Being a homeobox transcription factor, Prox1 has been shown to up-regulate the expression of lymphatic endothelial cell (LEC) markers, and to down-regulate blood vascular endothelial cell (BEC) markers in mature BECs (Hong *et al.*, 2002; Petrova *et al.*, 2002). These findings suggest that Prox1 regulates the program of differentiation of embryonic BECs to LECs by reprogramming the profiles of expression of specific markers of BECs and LECs. However, it is unclear which target genes elicit the functions of Prox1 during the process of lymphangiogenesis. Lymphangiogenesis is absent in the mice lacking some of Prox1 target genes including podoplanin and vascular endothelial growth factor receptor 3 (VEGFR3).

VEGFR3 serves as a receptor for lymphatic-specific VEGFs, VEGF-C and VEGF-D. VEGF-C is important for normal development of the lymphatic vessels, because deletion of *Vegf*

This article was published online ahead of print in *MBC in Press* (<http://www.molbiolcell.org/cgi/doi/10.1091/mbc.E06-09-0780>) on February 7, 2007.

  The online version of this article contains supplemental material at *MBC Online* (<http://www.molbiolcell.org>).

Address correspondence to: Kohei Miyazono (miyazono-ind@umin.ac.jp).

Abbreviations used: EC, endothelial cell; ESC, embryonic stem cell; PECAM1, platelet-endothelial cell adhesion molecule 1; SMA, α -smooth muscle actin; VEGF, vascular endothelial growth factor; BEC, blood vascular endothelial cell; LEC, lymphatic endothelial cell.

leads to complete absence of the lymphatic vasculature in mouse embryos (Karkkainen *et al.*, 2004). In *Vegfc*-null mice, LECs initially differentiate in the cardinal veins but fail to migrate and to form primary lymph sacs, suggesting that VEGF-C is an essential chemotactic and survival factor during embryonic lymphangiogenesis. *Vegfr3* deletion leads to defects in blood-vessel remodeling and embryonic death at midgestation, indicating its importance during early blood vascular development (Dumont *et al.*, 1998).

Recently, integrin $\alpha 9\beta 1$ was shown to function as a receptor for VEGF-C and VEGF-D (Vlahakis *et al.*, 2005). *Integrin* $\alpha 9$ -null mice die at 6–12 d of age from bilateral chylothorax, suggesting an underlying defect in lymphatic development (Huang *et al.*, 2000). Furthermore, integrin $\alpha 9$ was shown to be a target gene of the signals mediated by hepatocyte growth factor (HGF), which induces neo-lymphangiogenesis during tissue repair and inflammation (Kajiya *et al.*, 2005). Neo-lymphangiogenesis is also induced by two types of receptor tyrosine kinases, platelet-derived growth factor receptor β (PDGFR β), which serves as one of receptors for PDGF-BB (Cao *et al.*, 2004) and fibroblast growth factor receptor 3 (FGFR3), which serves as one of receptors for FGF-2 (Shin *et al.*, 2006). Notably, Prox1 has recently been shown to induce FGFR3 expression in BECs (Shin *et al.*, 2006).

Although various signaling cascades have been implicated in embryonic and/or adult lymphangiogenesis, their relationships with Prox1 remain largely unknown. Furthermore, although Prox1 has been shown to activate VEGF-C/VEGFR3 and FGF-2/FGFR3 signals, the direct effects of Prox1 on the behavior of ECs have not yet been elucidated. To address these questions, we expressed Prox1 in two types of ECs, mouse embryonic stem cell (ESC)-derived ECs and human umbilical venous endothelial cells (HUVECs). We found that Prox1 expression regulates the chemotaxis, sheet formation, and migration of ECs by modulating the expression of vascular and lymphatic signaling components and for the first time identified integrin $\alpha 9$ as a target gene of Prox1. Interestingly, our findings revealed that integrin $\alpha 9$ plays a pivotal role in sheet formation by and migration of LECs. These findings were confirmed in developing mouse embryos, suggesting their *in vivo* significance. Furthermore, knockdown of Prox1 expression in LECs resulted in decrease in the expression of VEGFR3 and integrin $\alpha 9$, leading to the decreased chemotaxis toward VEGF-C. These findings suggest that Prox1 alters the characteristics of BECs and maintains those of LECs by regulating multiple signaling cascades implicated in lymphangiogenesis.

MATERIALS AND METHODS

Cell Culture and Adenovirus Infection

Establishment of Tc-inducible ES cell lines from parental MGZ5TcH2 cells was as described (Masui *et al.*, 2005). Maintenance, differentiation, culture, and cell sorting of MGZ5 ES cells were as described (Yamashita *et al.*, 2000). VEGF-A (30 ng/ml), VEGF-C (300 ng/ml), PDGF-BB (10 ng/ml), and tetracycline (1 μ g/ml) were used in each experiment unless otherwise described. HUVECs were obtained from Sanko Junyaku and cultured as described (Ota *et al.*, 2002). Human dermal lymphatic endothelial cells (HDLECs) were obtained from Clonetics (San Diego, CA) and cultured in endothelial basal medium (EBM) containing 5% fetal bovine serum (FBS) and EC growth supplements (Clonetics). Recombinant adenoviruses with wild-type and mutant mouse Prox1 were generated and used as described (Fujii *et al.*, 1999).

RNA Interference and Oligonucleotides

Small interfering RNAs (siRNAs) were introduced into cells as described previously (Koinuma *et al.*, 2003). The target sequence for human Prox1 siRNA was 5'-CACCTTATTCGGGAAAGTCAA-3'. Control siRNAs were obtained from Ambion (Austin, TX).

Immunohistochemistry and Western Blot Analysis

Monoclonal antibodies to platelet-endothelial cell adhesion molecule 1 (PECAM1; Mec13.3) and α -smooth muscle actin (SMA; 1A4) for immunohistochemistry were purchased from BD PharMingen (San Diego, CA) and Sigma (St. Louis, MO), respectively. Staining of cultured cells was performed as described (Yamashita *et al.*, 2000). Stained cells were photographed using a phase-contrast microscope (Model IX70; Olympus, Melville, NY) or a confocal microscope (Model LSM510 META; Carl Zeiss MicroImaging, Thornwood, NY). All images were imported into Adobe Photoshop (San Jose, CA) as JPEGs or TIFFs for contrast manipulation and figure assembly. Antibodies to FLAG and α -tubulin for Western blot analysis and immunohistochemistry were obtained from Sigma. Antibodies to mouse VEGFR3, podoplanin, human VEGFR3, and Prox1 for Western blot analysis and immunohistochemistry were obtained from eBioscience (San Diego, CA), RDI (Flanders, NJ), Santa Cruz Biotechnology (Santa Cruz, CA), and Chemicon (Temecula, CA), respectively. Western blot analysis was performed as described (Kawabata *et al.*, 1998).

Fluorescence-activated Cell Sorting

To sort the LECs and BECs, we performed fluorescence-activated cell sorting (FACS) of mouse embryo cells with an FACS Vantage (Becton Dickinson, Mountain View, CA) as described previously (Morisada *et al.*, 2005). Briefly, E14 mouse embryos were dissociated and subjected to antibody staining for CD45-peridinin chlorophyll protein (PerCP) cyanine 5.5 (Cy5.5) to sort CD45-nonhematopoietic cells for further analysis. Subsequently, the cells were incubated with biotinylated anti-LYVE-1 antibodies (ALY7) followed by allophycocyanin-conjugated streptavidin (PharMingen, San Diego, CA). For double or triple staining, the cells were stained with CD31-phycoerythrin (PE)/FITC, CD34-PE (PharMingen), and TEK4-PE.14.

RNA Isolation and RT-PCR

Total RNA was prepared with ISOGEN reagent (Nippongene, Tokyo, Japan) according to the manufacturer's instructions and reverse-transcribed by random priming and a Superscript first-strand synthesis kit (Invitrogen, Carlsbad, CA). Quantitative RT-PCR analysis was performed using the GeneAmp 5700 Sequence Detection System (Applied Biosystems, Tokyo, Japan). The primer sequences and expected sizes of PCR products are available online as indicated in Supplementary Table 1.

Migration Assay

Chemotaxis was determined using a Cell Culture Insert (8- μ m pore size, BD Biosciences, San Jose, CA). A total of 5×10^4 cells were seeded in medium containing 0.5% serum in the upper chamber and migrated toward various growth factors as chemoattractants in the lower chamber for 4 h. When anti-integrin $\alpha 9\beta 1$ -neutralizing antibodies (Chemicon) were tested, cells were dissociated by trypsin/EDTA, incubated with neutralizing antibodies (30 μ g/ml), and seeded in the upper chamber. Cells in the upper chamber were carefully removed using cotton buds, and cells at the bottom of the membrane were fixed and stained with crystal violet 0.2%/methanol 20%. Quantification was performed by counting the stained cells. Assays were performed in triplicate at least three times.

Video Time-lapse Microscopy

Time-lapse imaging of migrating cells was performed on a Leica DM IRB microscope (Deerfield, IL) equipped with a hardware-controlled motor stage over 24 h in serum-reduced (0.5%) medium at 37°C/5% CO₂. Images were obtained with a Leica DC 350F CCD camera every 15 min and analyzed using Image J software (National Institutes of Health, Bethesda, MD). Migration of each cell was analyzed by measuring the distance traveled by a cell nucleus over the 24-h time period (Michl *et al.*, 2005). Average migration speed was calculated by analyzing at least 10 cells per group.

RESULTS

Prox1 Expression in ESC-derived ECs Induces Morphological Changes and Inhibits Sheet Formation

To examine the effects of Prox1 expression on embryonic ECs, we used an *in vitro* vascular differentiation system from mouse ESCs (Yamashita *et al.*, 2000). This system allows us to induce both endothelial and mural cells derived from common progenitors expressing VEGF receptor 2 (VEGFR2, Fik1). Because we wanted to induce the expression of Prox1 in differentiated ECs instead of undifferentiated ESCs, we established ESC lines carrying a tetracycline (Tc)-regulatable Prox1 transgene (Tc-Prox1) or no transgene (Tc-Empty; Supplementary Figure 1A; Masui *et al.*, 2005). Removal of Tc from culture of undifferentiated Tc-Prox1 cells, but

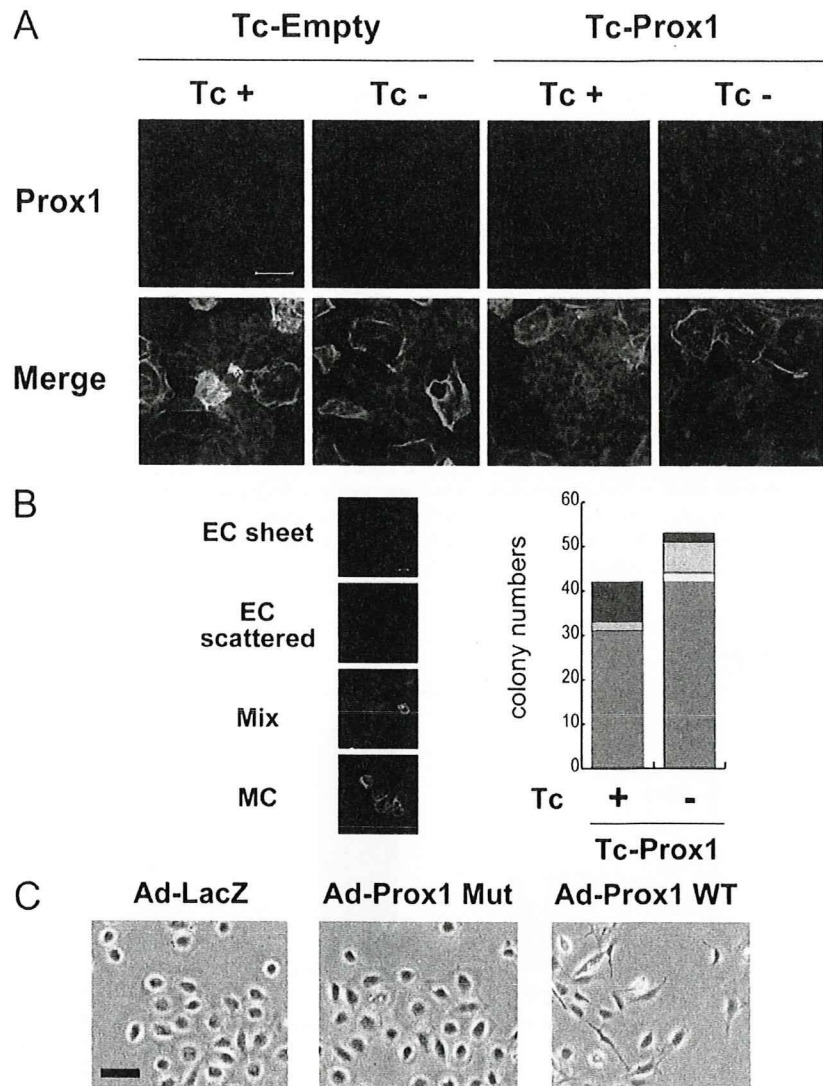


Figure 1. Effect of Tc-regulated Prox1 expression on the morphology and sheet formation of ESC-derived ECs and HUVECs. (A) Flk1+ endothelial progenitor cells were sorted from the differentiated ESCs carrying a Tc-regulated transgene encoding FLAG-epitope-tagged mouse Prox1 (Tc-Prox1) or control transgene (Tc-Empty) and redifferentiated in the presence (+) or absence (-) of Tc to obtain PECAM1-positive ECs (bottom, red) and smooth muscle α -actin (SMA)-positive mural cells (bottom, green). Expression of FLAG-Prox1 (top, blue) and the morphology and sheet formation of ECs (bottom, red) were examined. Scale bars, 100 μ m. (B) Quantitation of colony formation, EC and mural cell production, and endothelial sheet formation. Flk1+ cells derived from Tc-Prox1 ESCs were cultured sparsely with 10% fetal calf serum in the absence or presence of Tc for 4 d and stained for PECAM1 (red) and SMA (green). Numbers of different types of colonies per well were counted to determine the effects of Prox1 on colony formation of Flk1+ cells. Four colony types were observed: pure ECs forming sheet structures (EC-sheet, red); pure scattered ECs (EC-scattered, pink); pure mural cells (MC, green); and mixed colonies consisting of endothelial and mural cells (Mix, yellow). Experiments were repeated at least three times with essentially the same results. Bars, 50 μ m. (C) Morphology of HUVECs infected with adenoviruses encoding LacZ, DNA-binding mutant (Mut), or wild-type (WT) Prox1. Bars, 100 μ m.

not that of Tc-Empty cells, induced the expression of the FLAG epitope-tagged Prox1 gene (Supplementary Figure 1B).

To examine the effects of Prox1 expression on vascular development, we differentiated the Tc-Empty and Tc-Prox1 ES cells into Flk1-expressing (Flk1+) vascular progenitor cells in the presence of Tc, so that no transgene expression is induced. Flk1+ cells were sorted using anti-Flk1 antibodies and were redifferentiated in the presence or absence of Tc. As shown in Figure 1A, Prox1 transgene expression was induced in the vascular cells derived from Tc-Prox1 ES cells only in the absence of Tc. The level of Prox1 transgene expression in ESC-derived vascular cells was approximately twice as high as that of endogenous expression in the LECs derived from E14 mouse embryos (Supplementary Figure S1C). ESC-derived ECs formed a fine cobblestone-like structure of endothelial sheets when Prox1 was not expressed (Figure 1A). However, when Prox1 was expressed, ECs exhibited spindle shapes and failed to form sheet structures.

To further dissect the roles of Prox1 in endothelial sheet formation, we performed quantitative colony formation assays. When Flk1+ cells were plated at a lower density in the presence of VEGF-A, they formed four types of colonies emerging

from single Flk1+ cells (Yamashita *et al.*, 2000; Watabe *et al.*, 2003): PECAM1 (CD31)+ pure ECs with or without sheet structure (EC-sheet and EC-scattered, respectively), pure mural cells (MC), and mixtures of both (Mix; Figure 1B). Although the frequencies of pure EC colonies (EC-scattered and -sheet) were ~25% in the absence and presence of Prox1 expression, formation of endothelial sheets was significantly affected by Prox1 (Figure 1B). The frequency of sheet formation among pure endothelial colonies was 82% when single Flk1+ cells were cultured in the absence of Prox1. When Prox1 was expressed, most endothelial colonies exhibited scattered phenotypes (with a frequency of sheet formation of 22%). Furthermore, 95% of sheet-forming ECs derived from Tc-Prox1 ESCs failed to express Prox1 even in the absence of Tc (unpublished data), further suggesting that Prox1 expression in ESC-derived ECs inhibits sheet formation.

Prox1 Induces Morphological Changes and Inhibits Sheet Formation in HUVECs

We next examined whether Prox1 transgene expression also modulates the morphology and sheet formation of HUVECs, which are mature venous ECs. We used adenoviruses encod-

ing wild-type Prox1 (Ad-Prox1WT), a Prox1 mutant containing two amino acid substitutions in its DNA-binding domain (Ad-Prox1Mut) (Petrova *et al.*, 2002), and LacZ (Ad-LacZ) as controls. Levels of expression of wild-type and mutant Prox1 were shown to be comparable at moi 100 (Supplementary Figure 2A) when > 90% of HUVECs were infected (Supplementary Figure 2B). The level of Prox1 transgene expression was shown to be approximately three times as high as that of endogenous Prox1 expression in HDLECs (Supplementary Figure S2, B–D).

The morphology of and sheet formation by HUVECs were also affected by Prox1 (Figure 1C). Although HUVECs infected with adenoviruses encoding LacZ or mutant Prox1 formed a flat cobblestone-like structure, Prox1-expressing HUVECs were spindle-shaped and did not form sheet structures.

Prox1 Expression Increases Motility of ECs

Present findings that Prox1-expressing cells lose a cobblestone-like structure prompted us to examine the effects of Prox1 on the motility of ECs. Tracking single ECs using video time-lapse microscopy showed that Prox1 expression significantly increased the motility of ESC-derived ECs (Supplementary Videos 1 and 2 and Figure 2A) and HUVECs (Supplementary

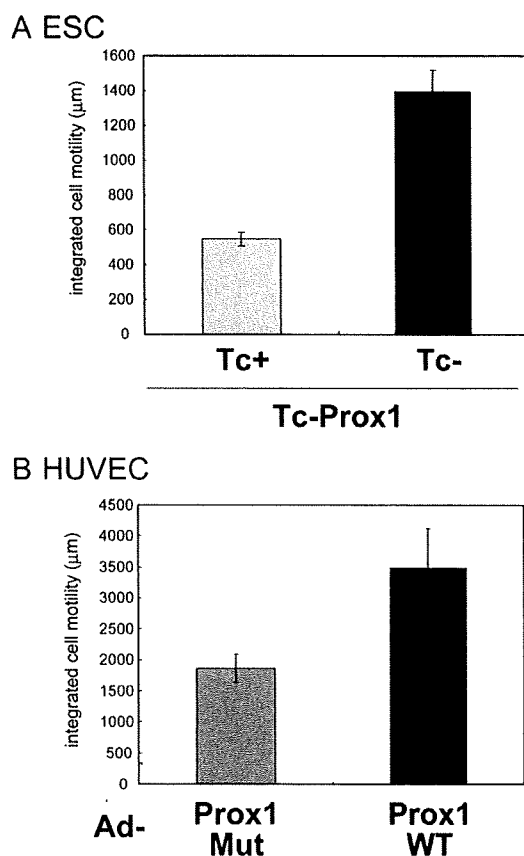


Figure 2. Effects of Prox1 on the migration of ESC-derived ECs and HUVECs. Cell migration was measured by video time-lapse microscopy as described in *Materials and Methods*. (A) ECs derived from Tc-Prox1 ESCs were subjected to video microscopy for 24 h (Supplementary Videos 1 and 2). (B) HUVECs were infected with adenoviruses (Ad) encoding DNA-binding mutant (Mut) or wild-type (WT) Prox1 and subjected to videomicroscopy for 24 h (Supplementary Videos 3 and 4). Results are expressed as the integrated cell motility over 24 h. Each value represents the mean of 10 determinations; bars, SD.

Videos 3 and 4 and Figure 2B). These findings suggest that Prox1 expression results in morphological changes of ECs, inhibition of sheet formation, and induction of EC motility, all of which may be critical phenomena for the progression of embryonic lymphangiogenesis.

Prox1 Increases Endothelial Motility via Induction of Integrin $\alpha 9$ Expression

We next examined the molecular mechanisms by which Prox1 regulates morphological changes of BECs. Petrova *et al.* (2002) reported that adenovirus-mediated Prox1 expression in human dermal microvascular endothelial cells (HDMECs) resulted in the down-regulation of BEC marker expression and up-regulation of LEC marker expression. We also found that the levels of transcripts for BEC markers (VE-cadherin and VEGFR2) and those for LEC markers (podoplanin and VEGFR3) were down- and up-regulated, respectively, only by Ad-Prox1WT infection in HUVECs, (Supplementary Figure 2), suggesting that Prox1 reprograms the vascular and lymphatic gene expression in HUVECs.

We then examined whether the activation of VEGFR3 signals by Prox1 mediates Prox1-induced morphological changes. However, inhibition of VEGFR3 signals in Prox1-expressing HUVECs by dominant-negative VEGFR3 mutants (Karkkainen *et al.*, 2000) failed to induce reversion of the Prox1-mediated phenotypes (Supplementary Figure 3), suggesting that VEGFR3 signaling is not directly involved in the induction of morphological changes of ECs by Prox1.

Recently, integrin $\alpha 9$, a member of the integrin family that is preferentially expressed in LECs (Petrova *et al.*, 2002), was shown to function as a receptor for VEGF-C and VEGF-D (Vlahakis *et al.*, 2005). Furthermore, *integrin $\alpha 9$ -null* mice exhibit defects in lymphatic systems (Huang *et al.*, 2000). Therefore, in order to examine the roles of integrin $\alpha 9$ in the Prox1-mediated morphological changes, we, for the first time, studied the roles of Prox1 in the regulation of integrin $\alpha 9$ expression. As shown in Figure 3, A and B, Prox1 expression increased the expression of integrin $\alpha 9$ in both ESC-derived ECs and HUVECs.

To elucidate the roles played by integrin $\alpha 9$ in the induction of phenotypic changes by Prox1, we used anti-human integrin $\alpha 9\beta 1$ neutralizing (function-blocking) antibodies. Reversion of the morphological changes and decreased sheet formation of HUVECs induced by Prox1 was observed with the addition of anti-integrin $\alpha 9$ -neutralizing antibodies to culture (Figure 3C). Furthermore, the increase in motility of HUVECs by Prox1 was lowered to basal level by anti-integrin $\alpha 9$ antibodies (Supplementary Videos 5–8 and Figure 3D). These findings suggest that the phenotypic changes of HUVECs induced by Prox1 are due to increased integrin $\alpha 9$ expression.

Prox1 Increases Chemotaxis to VEGF-C via Induction of Integrin $\alpha 9$ Expression

Because it was recently reported that VEGF-C and VEGF-D are ligands for integrin $\alpha 9\beta 1$ (Vlahakis *et al.*, 2005), we examined whether the up-regulation of integrin $\alpha 9$ expression by Prox1 contributed to the Prox1-induced increase in migration of ECs toward VEGF-C. Chamber migration assays showed that HUVECs expressing wild-type Prox1 migrated toward VEGF-C, and this migration was abrogated by anti- $\alpha 9\beta 1$ neutralizing antibody (Figure 3E), suggesting that Prox1 induces the migration of ECs toward VEGF-C by regulating the expression of integrin $\alpha 9$.

Prox1 Expression Inhibits Chemotaxis of BECs to VEGF-A and Promotes that to VEGF-C via Modulation of their Receptors

Although our findings suggest that signaling from VEGFR3 is not directly involved in Prox1-induced morphological changes

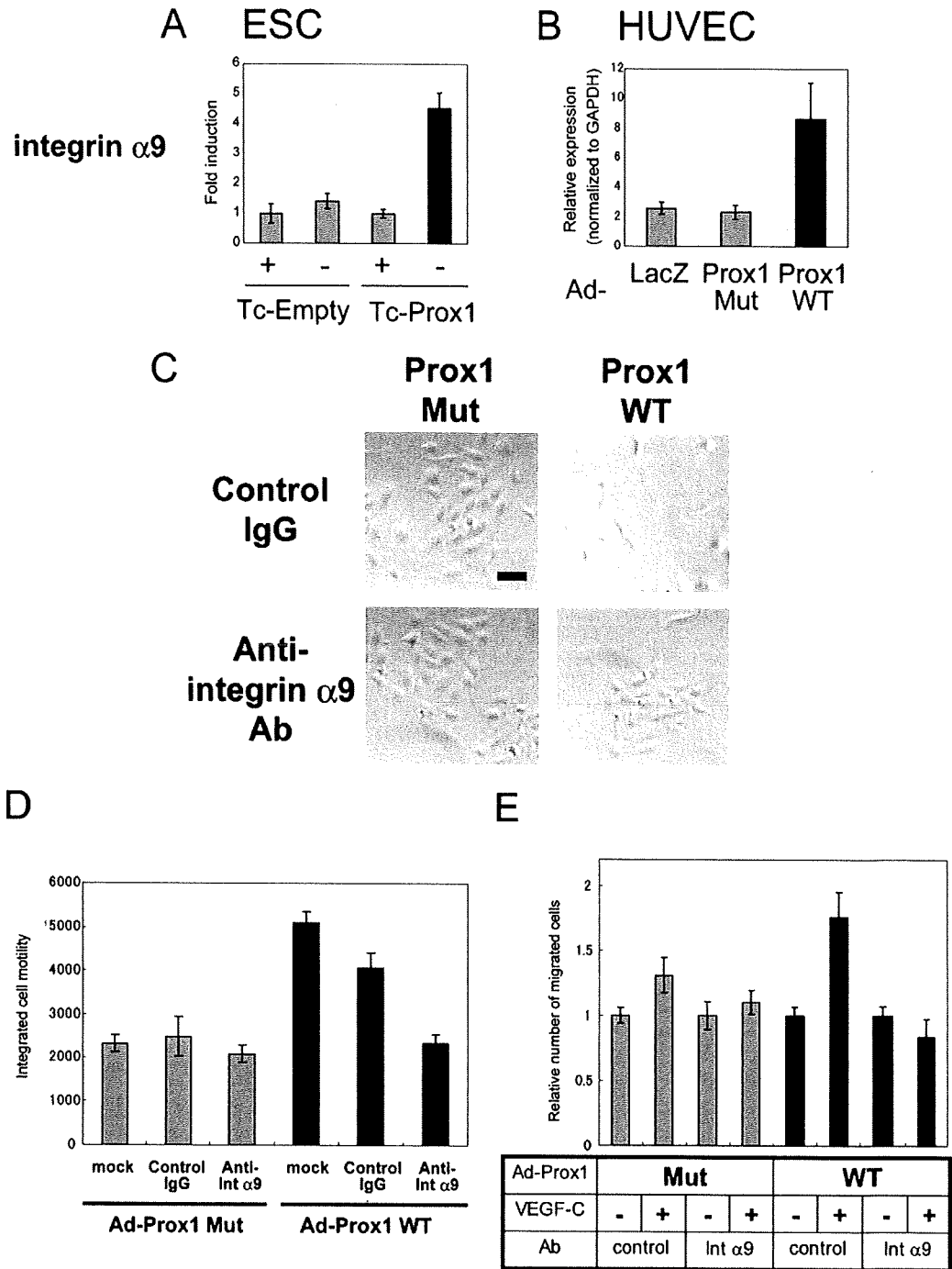


Figure 3. Roles of integrin $\alpha 9$ in the migration of HUVECs. (A and B) Expression of transcripts for integrin $\alpha 9$ was determined by quantitative real-time PCR analysis in ESC-derived ECs (A) and HUVECs (B). (C and D) HUVECs were infected with adenoviruses encoding DNA-binding mutant (Mut) or wild-type (WT) Prox1 and were subjected to videomicroscopy for 24 h in the presence of control IgG or anti-integrin $\alpha 9$ (int $\alpha 9$)-neutralizing antibodies. The final images of HUVECs (C) and integrated cell motility (D) are shown. Bars, 100 μ m. Each value represents the mean of 10 determinations; bars, SD (E) Cell migration was measured by Boyden chamber assay. HUVECs were infected with adenoviruses (Ad) encoding DNA-binding mutant (Mut) or wild-type (WT) and plated on Boyden chambers in the presence of control IgG or anti-integrin $\alpha 9$ (int $\alpha 9$)-neutralizing antibodies with VEGF-C placed in lower wells. Results are expressed as the ratio of number of migrated cells normalized to the control (no attractant). Each value represents the mean of triplicate determinations; bars, SD.

(Supplementary Figure 3), it may play important roles in other changes induced by Prox1 in ECs. BECs expressing VEGFR2

and LECs expressing VEGFR3 migrate preferentially toward their ligands VEGF-A and VEGF-C, respectively (Makinen *et*

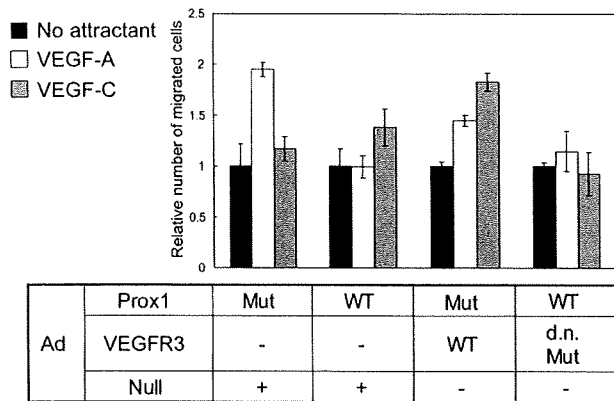


Figure 4. Effect of Prox1 on the migration of HUVECs stimulated with VEGF-A and VEGF-C. Cell migration was measured by Boyden chamber assay as described in *Materials and Methods*. HUVECs were infected with adenoviruses (Ad) encoding DNA-binding mutant (Mut) or wild-type (WT) Prox1 in combination with those encoding wild-type (WT), dominant-negative mutant form (d.n. Mut) of VEGFR3, or Null (encoding no transcripts) and plated on Boyden chambers with indicated chemoattractants placed in lower wells. Ad-Null was used in order to infect HUVECs with the same quantities of adenoviruses for all of samples. Results are expressed as the ratio of number of migrated cells normalized to control (no attractant). Each value represents the mean of triplicate determinations; bars, SD.

al., 2001). The alteration of expression of VEGFRs in HUVECs by Prox1 prompted us to study their chemoattraction toward VEGFs. Chamber migration assays showed that VEGF-A, but not VEGF-C, stimulated chemotaxis of the HUVECs expressing mutant Prox1 (Figure 4). In contrast, VEGF-C, but not VEGF-A, induced motility of those expressing wild-type Prox1. To examine whether Prox1 induces chemotaxis of HUVECs toward VEGF-C via up-regulation of VEGFR3 expression, we used adenoviruses encoding wild-type and dominant-negative forms of VEGFR3. Expression of wild-type VEGFR3 enhanced chemotaxis of HUVECs toward VEGF-C without altering their migration toward VEGF-A. In addition, inhibition of VEGFR3 signals by the dominant-negative VEGFR3 significantly decreased their chemotaxis toward VEGF-C, which was induced by Prox1. These findings suggest that Prox1 modulates endothelial chemotaxis toward VEGFs via its regulation of VEGFRs expression in addition to that of integrin $\alpha 9$.

Expression of VEGFR3 and Integrin $\alpha 9$ Is Increased in Prox1-expressing LECs from Mouse Embryos

To examine the *in vivo* significance of our finding that Prox1 induces the expression of VEGFR3 and integrin $\alpha 9$ in ESC-derived ECs, we compared their expression in LECs and BECs derived from E14 mouse embryos. We previously raised monoclonal antibodies against a LEC marker, LYVE-1, and found that sorted CD45-CD31+CD34-lowLYVE-1+ cells derived from E14 mouse embryos represent LECs and that CD45-CD31+CD34+LYVE-1- cells represent BECs (Morisada *et al.*, 2005). We confirmed that expression of LYVE-1 and Prox1 was detected only in sorted LECs (Figure 5). We further examined the expression of Prox1 target genes in LECs and BECs. Expression of VEGFR3 and integrin $\alpha 9$ was detected in the cells in both the LEC and BEC fractions, and their levels of expression in LEC were higher than those in BECs. These findings together suggest that the *in vitro* induction by Prox1 of expression of VEGFR3 and integrin $\alpha 9$ may mimic the process of embryonic lymphangiogenesis.

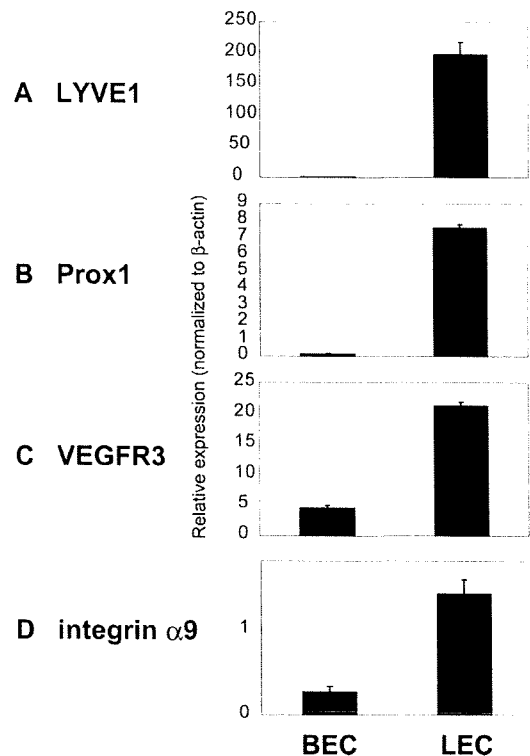


Figure 5. Expression of BEC and LEC markers in Prox1-expressing LECs derived from mouse embryos. E14 mouse embryos were dissected, and embryonic liver and spleen were removed. Other tissues were dissociated and subject to FACS sorting with anti-CD45, LYVE1 (ALY7), CD31, and CD34 antibodies (see *Materials and Methods*). CD45-; CD31+; CD34-; LYVE1- BEC fractions and CD45-; CD31+; CD34-; LYVE1+ LEC fractions were analyzed for the expression of transcripts for LYVE1 (A), Prox1 (B), VEGFR3 (C), and integrin $\alpha 9$ (D) by quantitative real-time PCR analysis. Each value represents the mean of triplicate determinations; bars, SD.

Prox1 Knockdown in LECs Modulates Expression of Lymphatic Endothelial Markers and their Cellular Behavior

Prox1 expression is initiated during embryonic lymphangiogenesis and is maintained in mature LECs, prompting us to examine whether knockdown of Prox1 expression in mature LEC affects their characteristics.

We detected endogenous Prox1 protein in the nuclei of HDLECs, whereas no Prox1 protein was detected in HUVECs (Figure 6A). Expression of transcripts for Prox1, VEGFR3, and integrin $\alpha 9$ was significantly higher in HDLECs than in HUVECs (unpublished data). We next decreased Prox1 levels with siRNAs (Figure 6, B and C). siRNA-mediated decrease of Prox1 led to decrease in the expression of various target genes of Prox1, such as VEGFR3, and integrin $\alpha 9$ (Figure 6, D and E), whereas the expression of most genes including GAPDH was not affected, suggesting that Prox1 maintains the expression of LEC markers in HDLECs.

Mature LECs have been reported to migrate toward VEGF-C (Makinen *et al.*, 2001). To study the effects of Prox1 knockdown on the behavior of HDLECs, we examined their chemotaxis toward VEGFs (Figure 6F). Although HDLECs migrate toward VEGF-A and VEGF-C, Prox1 knockdown caused a specific decrease in the chemotaxis toward VEGF-C (Figure 6F). These results suggest that Prox1 maintains the characteristics of LECs by sustaining the expression of LEC markers.

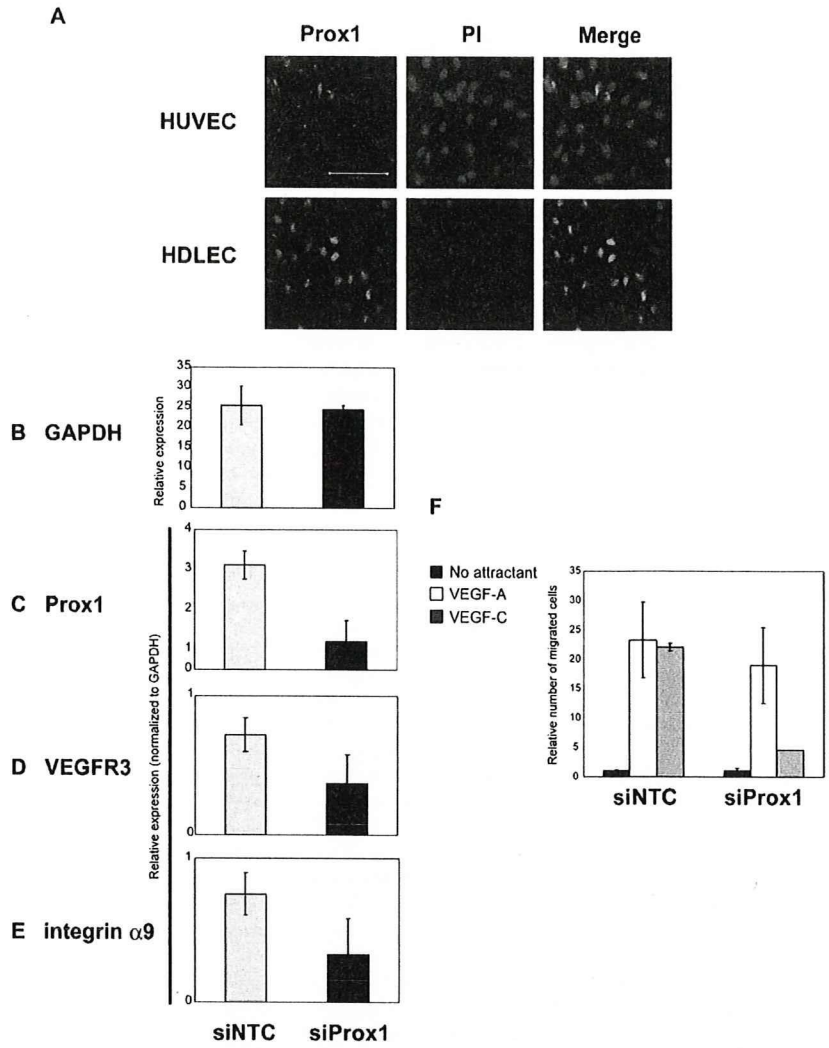


Figure 6. Roles of endogenous Prox1 in HDLECs. (A) Expression of endogenous Prox1 (left; green) was examined by specific antibodies in HUVECs (top) and HDLECs (bottom), with counterstaining for nuclei with propidium iodide (PI, middle; red; and right, merge). Bars, 100 μm . (B–E) Effects of Prox1 knockdown on expression of GAPDH (B), Prox1 (C), VEGFR3 (D), and integrin $\alpha 9$ (E) were examined by quantitative real-time PCR analysis. A scrambled siRNA sequence (Ambion) was used as a negative control siRNA (siNTC). Each value represents the mean of triplicate determinations; bars, SD. (F) Effects of Prox1 knockdown on the chemotaxis of HDLECs toward VEGF-A (50 ng/ml) and VEGF-C (50 ng/ml). Cell migration was measured by Boyden chamber assay as described in *Materials and Methods*. HDLECs were transfected with scrambled siRNAs (siNTC) or Prox1 siRNAs and plated on Boyden chambers with indicated chemoattractants placed in the lower wells. Results are expressed as the ratio of number of migrated cells normalized to control (no attractant). Each value represents the mean of triplicate determinations; bars, SD.

DISCUSSION

Recent studies have revealed that lymphangiogenesis is regulated by various signaling cascades mediated by VEGFs/VEGFRs (Dumont *et al.*, 1998; Karkkainen *et al.*, 2000; Suzuki *et al.*, 2005), and integrin $\alpha 9\beta 1$ (Huang *et al.*, 2000). The present study showed that expression of Prox1 in ECs regulates the expression of various signaling components, including integrin $\alpha 9$, VEGFR2, and VEGFR3, leading to alteration of chemotaxis, sheet formation, and migration of ECs. We also observed that Prox1 modulates the signaling pathways mediated by angiopoietins/Tie2 (Morisada *et al.*, 2005) and FGF/FGFR3 (Shin *et al.*, 2006) in both ESC-derived ECs and HUVECs (unpublished data). In addition, because integrin $\alpha 9$ has been implicated in modulation of signaling cascades mediated by HGF (Kajiya *et al.*, 2005), Prox1 may indirectly modulate HGF signaling. These findings, together with those of previous studies, suggest that Prox1 is a master transcription factor that induces the differentiation of ECs into LECs via regulation of multiple signaling cascades that play important roles in lymphangiogenesis.

Interestingly, we have found that Prox1 induces growth of Flk1+ ECs derived from ESCs, but inhibits the growth of

undifferentiated ESCs (unpublished data). These findings suggest that Prox1 requires cell-type-specific modulators for its transcriptional activities and further imply the importance of choosing appropriate endothelial cell types in the identification of Prox1 target genes during embryonic lymphatic differentiation. Although previous studies used mature human dermal ECs to identify target genes of Prox1 (Hong *et al.*, 2002; Petrova *et al.*, 2002), it will be of great interest to use ESC-derived ECs for this purpose.

Alteration of endothelial signaling cascades by Prox1 resulted in decrease in sheet formation, increased motility, and down- and up-regulation of chemotaxis toward VEGF-A and VEGF-C, respectively. An important question is whether these changes mimic the differentiation from BECs to LECs. Blood vascular endothelium and lymphatic endothelium differ in certain specific morphological characteristics. For example, the lymphatic capillaries are larger than the blood capillaries and have an irregular or collapsed lumen, a discontinuous basal lamina, overlapping intercellular junctional complexes, and anchoring filaments that connect the LECs to the extracellular matrix (Witte *et al.*, 2001). The results of morphological observation of in vitro cultured BECs and LECs are controversial. Makinen *et al.* (2001) reported that LECs sorted from human dermal microvascular cells using anti-VEGFR3 antibodies ex-

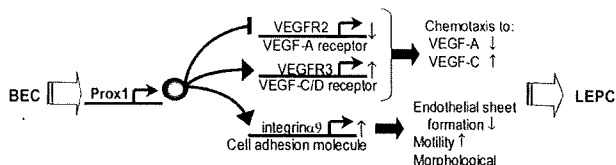


Figure 7. Schematic representation of the roles of Prox1 during the differentiation of blood vessel ECs (BECs) to lymphatic endothelial progenitor cells (LEPCs). See text for details.

hibit elongated cell shapes in the presence of VEGF-C compared with the BECs sorted from the same source. However, Kriehuber *et al.* (2001) reported that LECs sorted from dermal cell suspensions using anti-podoplanin antibodies were not morphologically distinguishable from the BECs sorted from the same source. These differences in findings may be explained by the differences in methods used to isolate and culture LECs and BECs.

During embryonic lymphangiogenesis, Prox1-expressing ECs sprout from cardinal veins and migrate toward VEGF-C-expressing mesenchymal cells (Oliver, 2004). These observations suggest that Prox1-expressing cells need to be mobile to form primary lymphatic sacs. In addition, Prox1 induces proliferation of ESC-derived ECs and HUVECs (unpublished data). However, such cells become stabilized in the VEGF-C-expressing region and form lymphatic capillaries. Furthermore, present work showed that the morphological changes of ECs induced by Prox1 is not dependent on VEGFR3 (Supplementary Figure S3), but on integrin α 9 (Figure 3) and that the enhanced chemotaxis toward VEGF-C requires VEGFR3 and integrin α 9 (Figures 3 and 4). These findings suggest the hypothesis that Prox1 activates ECs by inducing integrin α 9 expression, which results in chemotaxis toward VEGF-C in collaboration with VEGFR3, expression of which is also induced by Prox1, and stabilizes and induces maturation of them via signals mediated mainly by VEGF-C/VEGFR3. This hypothesis is supported by the observation that survival of mature LECs was inhibited by Prox1 knockdown (unpublished data). Prox1 thus appears to function as a master transcription factor for lymphangiogenesis, playing key roles in most of the critical steps during the development of lymphatic sacs, including mobilization, migration, and proliferation of LECs, as well as stabilization of lymphatic capillaries, through modulation of multiple signaling cascades (Figure 7).

The lymphatic vasculature plays important roles in the pathogenesis of various conditions and diseases such as lymphedema and cancer metastasis. The findings of the present study suggest the possibility that expression of Prox1 in BECs and/or endothelial progenitor cells derived from patients may be useful as a therapeutic strategy in regenerative medical treatment of lymphedema. Alternatively, knockdown of Prox1 in cancer patients may inhibit tumor lymphangiogenesis and prevent metastasis.

ACKNOWLEDGMENTS

We thank Drs. J. Yamashita, H. Miki, S. Nishikawa, and members of Department of Molecular Pathology of the University of Tokyo for discussion. This research was supported by Grants-in-Aid for Scientific Research from the Ministry of Education, Science, Sports, and Culture of Japan.

REFERENCES

Cao, R. *et al.* (2004). PDGF-BB induces intratumoral lymphangiogenesis and promotes lymphatic metastasis. *Cancer Cell* 6, 333–345.

Dumont, D. J., Jussila, L., Taipale, J., Lymboussaki, A., Mustonen, T., Pajusola, K., Breitman, M., and Alitalo, K. (1998). Cardiovascular failure in mouse embryos deficient in VEGF receptor-3. *Science* 282, 946–949.

Fujii, M., Takeda, K., Imamura, T., Aoki, H., Sampath, T. K., Enomoto, S., Kawabata, M., Kato, M., Ichijo, H., and Miyazono, K. (1999). Roles of bone morphogenetic protein type I receptors and Smad proteins in osteoblast and chondroblast differentiation. *Mol. Biol. Cell* 10, 3801–3813.

Hong, Y. K., Harvey, N., Noh, Y. H., Schacht, V., Hirakawa, S., Detmar, M., and Oliver, G. (2002). Prox1 is a master control gene in the program specifying lymphatic endothelial cell fate. *Dev. Dyn.* 225, 351–357.

Huang, X. Z., Wu, J. F., Ferrando, R., Lee, J. H., Wang, Y. L., Farese, R. V., Jr., and Sheppard, D. (2000). Fatal bilateral chylothorax in mice lacking the integrin α 9 β 1. *Mol. Cell. Biol.* 20, 5208–5215.

Kajiyama, K., Hirakawa, S., Ma, B., Drinnenberg, I., and Detmar, M. (2005). Hepatocyte growth factor promotes lymphatic vessel formation and function. *EMBO J.* 24, 2885–2895.

Karkkainen, M. J., Ferrell, R. E., Lawrence, E. C., Kimak, M. A., Levinson, K. L., McTigue, M. A., Alitalo, K., and Finegold, D. N. (2000). Missense mutations interfere with VEGFR-3 signalling in primary lymphoedema. *Nat. Genet.* 25, 153–159.

Karkkainen, M. J. *et al.* (2004). Vascular endothelial growth factor C is required for sprouting of the first lymphatic vessels from embryonic veins. *Nat. Immunol.* 5, 74–80.

Karpanen, T., and Alitalo, K. (2001). Lymphatic vessels as targets of tumor therapy? *J. Exp. Med.* 194, F37–F42.

Kawabata, M., Inoue, H., Hanyu, A., Imamura, T., and Miyazono, K. (1998). Smad proteins exist as monomers *in vivo* and undergo homo- and hetero-oligomerization upon activation by serine/threonine kinase receptors. *EMBO J.* 17, 4056–4065.

Kriehuber, E., Breiteneder-Geleff, S., Groeger, M., Soleiman, A., Schoppmann, S. F., Stingl, G., Kerjaschki, D., and Maurer, D. (2001). Isolation and characterization of dermal lymphatic and blood endothelial cells reveal stable and functionally specialized cell lineages. *J. Exp. Med.* 194, 797–808.

Koinuma, D. *et al.* (2003). Arkadia amplifies TGF- β superfamily signalling through degradation of Smad7. *EMBO J.* 22, 6458–6470.

Makinen, T. *et al.* (2001). Isolated lymphatic endothelial cells transduce growth, survival and migratory signals via the VEGF-C/D receptor VEGFR-3. *EMBO J.* 20, 4762–4773.

Masui, S., Shimamoto, D., Toyooka, Y., Yagi, R., Takahashi, K., and Niwa, H. (2005). An efficient system to establish multiple embryonic stem cell lines carrying an inducible expression unit. *Nucleic Acids Res.* 33, e43.

Michl, P. *et al.* (2005). CUTL1 is a target of TGF β signaling that enhances cancer cell motility and invasiveness. *Cancer Cell* 7, 521–532.

Morisada, T. *et al.* (2005). Angiopoietin-1 promotes LYVE-1-positive lymphatic vessel formation. *Blood* 105, 4649–4656.

Oliver, G. (2004). Lymphatic vasculature development. *Nat. Rev. Immunol.* 4, 35–45.

Ota, T., Fujii, M., Sugizaki, T., Ishii, M., Miyazawa, K., Aburatani, H., and Miyazono, K. (2002). Targets of transcriptional regulation by two distinct type I receptors for transforming growth factor- β in human umbilical vein endothelial cells. *J. Cell. Physiol.* 193, 299–318.

Petrova, T. V., Makinen, T., Makela, T. P., Saarela, J., Virtanen, I., Ferrell, R. E., Finegold, D. N., Kerjaschki, D., Yla-Herttuala, S., and Alitalo, K. (2002). Lymphatic endothelial reprogramming of vascular endothelial cells by the Prox-1 homeobox transcription factor. *EMBO J.* 21, 4593–4599.

Shin, J. W., Min, M., Larrieu-Lahargue, F., Canron, X., Kunstfeld, R., Nguyen, L., Henderson, J. E., Bikfalvi, A., Detmar, M., and Hong, Y. K. (2006). Prox1 promotes lineage-specific expression of fibroblast growth factor (FGF) receptor-3 in lymphatic endothelium: a role for FGF signaling in lymphangiogenesis. *Mol. Biol. Cell* 17, 576–584.

Suzuki, H., Watabe, T., Kato, M., Miyazawa, K., and Miyazono, K. (2005). Roles of vascular endothelial growth factor receptor 3 signaling in differentiation of mouse embryonic stem cell-derived vascular progenitor cells into endothelial cells. *Blood* 105, 2372–2379.

Vlahakis, N. E., Young, B. A., Atakilit, A., and Sheppard, D. (2005). The lymphangiogenic vascular endothelial growth factors VEGF-C and -D are ligands for the integrin α 9 β 1. *J. Biol. Chem.* 280, 4544–4552.

Watabe, T., Nishihara, A., Mishima, K., Yamashita, J., Shimizu, K., Miyazawa, K., Nishikawa, S., and Miyazono, K. (2003). TGF- β receptor kinase inhibitor enhances growth and integrity of embryonic stem cell-derived endothelial cells. *J. Cell Biol.* 163, 1303–1311.

Wigle, J. T., and Oliver, G. (1999). Prox1 function is required for the development of the murine lymphatic system. *Cell* 98, 769-778.

Wigle, J. T., Harvey, N., Detmar, M., Lagutina, I., Grosveld, G., Gunn, M. D., Jackson, D. G., and Oliver, G. (2002). An essential role for Prox1 in the induction of the lymphatic endothelial cell phenotype. *EMBO J.* 21, 1505-1513.

Witte, M. H., Bernas, M. L., Martin, C. P., and Witte, C. L. (2001). Lymphangiogenesis and lymphangiodysplasia: from molecular to clinical lymphology. *Microsc. Res. Tech.* 55, 122-145.

Yamashita, J., Itoh, H., Hirashima, M., Ogawa, M., Nishikawa, S., Yurugi, T., Naito, M., Nakao, K., and Nishikawa, S. (2000). Flk1-positive cells derived from embryonic stem cells serve as vascular progenitors. *Nature* 408, 92-96.

Activin-Nodal signaling is involved in propagation of mouse embryonic stem cells

Kazuya Ogawa^{1,*}, Akira Saito^{2,*}, Hisanori Matsui¹, Hiroshi Suzuki², Satoshi Ohtsuka¹, Daisuke Shimosato^{1,3}, Yasuyuki Morishita², Tetsuro Watabe², Hitoshi Niwa^{1,3,†} and Kohei Miyazono^{2,4,‡}

¹Laboratory for Pluripotent Cell Studies, RIKEN Center for Developmental Biology, 2-2-3 Minatojima-Minamimachi, Chuo-ku, Kobe 650-0047, Japan

²Department of Molecular Pathology, Graduate School of Medicine, University of Tokyo, 7-3-1 Hongo, Bunkyo-ku, Tokyo 113-0033, Japan

³Department of Developmental and Regenerative Medicine, Graduate School of Medicine, Kobe University, 7-5-1, Kusunokicho, Chuo-ku, Kobe 650-0017, Japan

⁴Department of Biochemistry, The Cancer Institute of the Japanese Foundation for Cancer Research, Toshima-ku, Tokyo 170-8455, Japan

*These authors contributed equally to this work

†Authors for correspondence (e-mail: niwa@cdb.riken.jp; miyazono-ind@umin.ac.jp)

Accepted 10 October 2006

Journal of Cell Science 120, 55-65 Published by The Company of Biologists 2007

doi:10.1242/jcs.03296

Summary

Embryonic stem (ES) cells are self-renewing cells that maintain pluripotency to differentiate into all types of cells. Because of their potential to provide a variety of tissues for use in regenerative medicine, there is great interest in the identification of growth factors that govern these unique properties of ES cells. However, the signaling pathways controlling ES cell proliferation remain largely unknown. Since transforming growth factor β (TGF β) superfamily members have been implicated in the processes of early embryogenesis, we investigated their roles in ES cell self-renewal. Inhibition of activin-Nodal-TGF β signaling by Smad7 or SB-431542 dramatically decreased ES cell proliferation without decreasing ES pluripotency. By contrast, inhibition of bone morphogenetic protein (BMP) signaling by Smad6 did not exhibit such effects, suggesting that activin-Nodal-TGF β signaling, but not BMP signaling, is indispensable for ES cell propagation. In serum-free

culture, supplementation of recombinant activin or Nodal, but not TGF β or BMP, significantly enhanced ES cell propagation without affecting pluripotency. We also found that activin-Nodal signaling was constitutively activated in an autocrine fashion in serum-free cultured ES cells, and that inhibition of such endogenous signaling by SB-431542 decreased ES cell propagation in serum-free conditions. These findings suggest that endogenously activated autocrine loops of activin-Nodal signaling promote ES cell self-renewal.

Supplementary material available online at <http://jcs.biologists.org/cgi/content/full/120/1/55/DC1>

Key words: Embryonic stem cell, Self-renewal, Propagation, TGF β superfamily signaling, Activin-Nodal, Serum-free

Introduction

One of the most important characteristics of stem cells is their ability to self-renew. Self-renewal is achieved by suppression of differentiation and stimulation of proliferation. Embryonic stem (ES) cells are self-renewing cells derived from the inner cell mass (ICM) of blastocysts (Niwa, 2001). They have the ability to maintain pluripotency to differentiate into all types of cells of the three germ layers, and are expected to be of great use in regenerative medicine. The signaling instructions that govern these characteristics are provided by growth factors in the stem cell niche microenvironment (Schofield, 1978). Identification of these growth factors and extending such knowledge to control ES cell propagation would improve understanding of the basic biology of ES cells and may yield therapeutic benefits in regenerative medicine. However, the signaling pathways that govern the proliferation of ES cells remain largely unknown.

At present, mouse ES (mES) cells can be propagated in medium containing fetal calf serum (FCS) and cytokine leukemia inhibitory factor (LIF) without the support of feeder cells (Smith et al., 1988; Niwa, 2001). The effect of LIF is

mediated through a cell-surface complex composed of LIFR β and gp130. Upon ligand binding, gp130 activates Janus-associated tyrosine kinases (JAK) and their downstream component signal transducer and activator of transcription (STAT)-3. Although activation of STAT3 is necessary and sufficient for suppression of differentiation of mES cells (Niwa et al., 1998; Matsuda et al., 1999), LIF does not appear to regulate the proliferation of mES cells directly (Raz et al., 1999; Viswanathan et al., 2002). These findings suggest that unidentified growth factors provided by serum or feeder cells and/or in an autocrine fashion by ES cells could contribute to self-renewal of ES cells.

Several lines of evidence suggest that the signaling pathways mediated by the members of the transforming growth factor β (TGF β) superfamily play important roles in the biology of epiblasts and ES cells. The TGF β superfamily includes nearly 30 proteins in mammals, e.g. TGF β , activin, Nodal and bone morphogenetic proteins (BMPs), and its members have a broad array of biological activities. Members of the TGF β superfamily signal via heteromeric complexes of type I and type II receptors (Heldin et al., 1997). Upon ligand binding,

the constitutively active type II receptor kinase phosphorylates the type I receptor which, in turn, activates intracellular signaling cascades including Smad pathways. Activins, TGF β s and Nodal bind to type I receptors known as activin receptor-like kinase (ALK)-4, ALK-5 and ALK-7, respectively. In addition, Cripto serves as a co-receptor for Nodal in conjunction with ALK-4. The activated type I receptors phosphorylate receptor-regulated Smad proteins (R-Smads). Smad2 and Smad3 transduce signals for TGF β , activin and Nodal, whereas Smad1, Smad5 and Smad8 are activated by BMP type I receptors (Massague, 1998). Activated R-Smads form complexes with common-partner Smad (Co-Smad, i.e. Smad4), translocate into the nucleus, and regulate the expression of target genes in cooperation with various transcription factors such as those of the FAST-FoxH family. Smad6 and Smad7 are inhibitory Smads (I-Smads) (Imamura et al., 1997; Nakao et al., 1997), and have been reported to exhibit significant differences in the manner of inhibition of TGF β superfamily signaling. BMP signaling is inhibited by both Smad6 and Smad7, whereas activin-Nodal-TGF β signaling is more potently inhibited by Smad7 (Hata et al., 1998; Itoh et al., 1998; Hanyu et al., 2001).

Genetic studies have shown that embryos deficient in *Smad4* display defective epiblast proliferation and retarded ICM outgrowth (Sirard et al., 1998), and that *Nodal* null mice display very little *Oct3/4* expression and substantial reduction in size of the epiblast cell population (Conlon et al., 1994; Robertson et al., 2003). Furthermore, large-scale gene profiling of embryonic and adult stem cells has revealed that TGF β signaling networks are likely to play important roles in maintenance of the unique properties of ES cells (Ramalho-Santos et al., 2002; Ivanova et al., 2002; Brandenberger et al., 2004). Nodal signaling, in particular, has been speculated to be active in undifferentiated human ES (hES) cells, since components of Nodal signals (human orthologs of *Cripto* and *FAST1*) and a target gene (a human homolog of *Lefty2*) are transcriptionally enriched (Brandenberger et al., 2004). Moreover, phosphorylation and the nuclear localization of Smad2/3 were detected in undifferentiated hES cells and shown to play important roles in maintenance of their pluripotency (James et al., 2005). However, the precise roles of Smad2/3 signaling mediated by activin-Nodal-TGF β in self-renewal of mouse and human ES cells have yet to be elucidated.

In the present study, we investigated the effects of TGF β superfamily members on mES cell self-renewal. When activin-Nodal-TGF β signaling was inhibited by Smad7 expression or the specific inhibitor SB-431542, mES cell propagation was dramatically decreased, whereas inhibition of BMP signaling by Smad6 expression did not. In clonal cultures with serum-free medium, supplementation of recombinant Nodal and activin increased the ES cell proliferation ratio with maintenance of the pluripotent state, but supplementation with BMP-4 did not. These findings indicate that Nodal and activin signaling promotes mES cell propagation, and that mES cells themselves produce this activity.

Results

Inhibition of activin-Nodal-TGF β signaling decreases mES cell proliferation

To study the roles of TGF β superfamily signaling in the

proliferation of ES cells cultured in FCS-containing medium, we first used various natural inhibitors such as Smad6 and 7. We confirmed the specificity of TGF β superfamily signaling, which is inhibited by Smad6 and Smad7 in MGZ5 ES cells, with luciferase reporter assays using BMP-specific Id-1-luc and activin-Nodal-specific activin responsive elements (ARE)-luc (Chen et al., 1996; Korchynskyi and ten Dijke, 2002). Transient expression of Smad6 inhibited BMP-dependent reporter activity, whereas that of Smad7 inhibited both BMP-dependent and activin-Nodal-TGF β -dependent reporter activities (Fig. 1A). These results suggested that the pathway specificity of inhibitory Smads is conserved in mES cells, and that BMP and activin-Nodal-TGF β signaling is autonomously activated in mES cells in FCS-containing medium.

To examine the effects of inhibition of BMP and activin-Nodal-TGF β signaling on self-renewal of mES cells, we overexpressed mouse *Smad6* or *Smad7* using an episomal vector system, which allows efficient transfection and strong expression of transgenes. *Smad6* and *Smad7* cDNAs were introduced into pCAG-IP supertransfection vector and then transfected into MGZ5 ES cells. Quantitative RT-PCR analysis showed that expression of Smad7 was nine times higher in the Smad7-transfected cells than in the control (supplementary material Fig. S1A). Forced expression of *Smad7* significantly reduced cell number and colony size after culture in FCS-containing medium, whereas that of *Smad6* yielded a smaller reduction of cell number and colony size compared with empty transfectants (Fig. 1B-D). We also calculated the cell number per colony to determine the relative proliferation. Forced expression of *Smad7* decreased the ES cell proliferation ratio by about 75%, whereas that of *Smad6* decreased ES cell proliferation ratio by only 10%, which was not significant (Fig. 1D).

To examine whether the growth-inhibitory effect of Smad7 is due to inhibition of activin-Nodal-TGF β signaling, we blocked the same signal pathway with SB-431542, a synthetic molecule that inhibits the kinases of receptors for activin-Nodal-TGF β but not those of BMPs (Laping et al., 2002; Inman et al., 2002). The size of colonies without inhibition of TGF β signaling was larger than that of colonies of mock transfectants in episomal transfection, possibly because of the absence of drug (puromycin) selection (Fig. 1B and Fig. 2A). Addition of 10 μ M SB-431542 to FCS-containing medium significantly inhibited mES cell proliferation (Fig. 2). However, SB-431542 did not reduce the cell number as strongly as forced expression of Smad7, which may inhibit the plating efficiency of mES cells. These results strongly suggest that autonomously activated activin-Nodal-TGF β signaling, not BMP signaling, contributes to proliferation of mES cells in FCS-containing medium.

The growth-inhibitory effect of Smad7 is reversible

We further examined whether growth inhibition by *Smad7* expression affects the characteristics of mES cells, using a reversible *Smad7* expression system. As shown in Fig. 3A, fSmad7-10⁺ ES cells were generated by stable integration of the floxed-*Smad7* cDNA transgene into EB3 ES cells. fSmad7-10⁺ ES cells expressing five times as many *Smad7* transcripts as the control cells (supplementary material Fig. S1B), but not the *DsRed* transgene, were cultured in FCS-containing medium with 1 μ g/ml puromycin for 1 month, and then transfected with

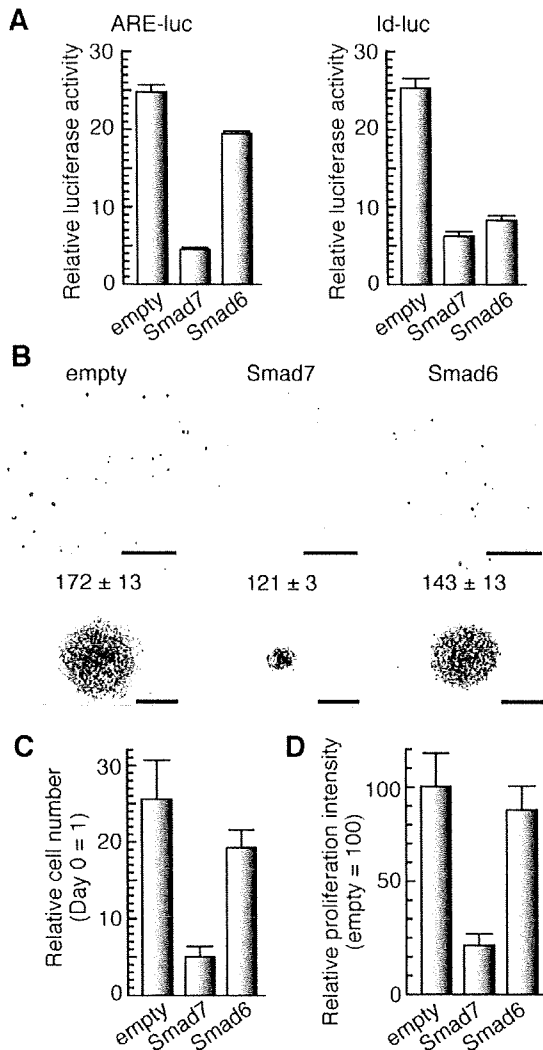


Fig. 1. Forced Smad7 expression inhibited ES cell propagation. (A) Luciferase reporter assay in MGZ5 cells transfected with reporter constructs (ARE-luc reporter or Id-1-luc reporter) and each expression plasmid. Each bar represents the mean ± s.e.m. ($n=3$). (B) Colony morphologies of supertransfectants. MGZ5 cells were transfected with Smad7-expressing plasmid (middle), Smad6 plasmid (right), or empty vector (left), seeded at 2000 cells/well in six-well plates, and cultured for 1 week in medium supplemented with puromycin. Numbers indicate numbers of colonies appearing ($n=3$). The lower panel shows AP staining. Bars, 5 mm (upper panels); 200 μ m (lower panels). (C) Relative numbers of each transfectant present on Day 7 of culture compared with that at Day 0. Each bar represents the mean ± s.e.m. ($n=3$). (D) Relative proliferation intensity is shown as total cell number/number of colonies appearing, compared with that of empty vector transfectants (100%). Each bar represents the mean ± s.e.m. ($n=3$).

pCAGGS-Cre. Cre-mediated recombination resulted in the generation of fSmad7-10⁻ ES cells, in which the *Smad7* transgene had been excised and the *DsRed* transgene activated (Fig. 3A,B). Excision of the *Smad7* transgene was confirmed by RT-PCR analysis (supplementary material Fig. S1B), which

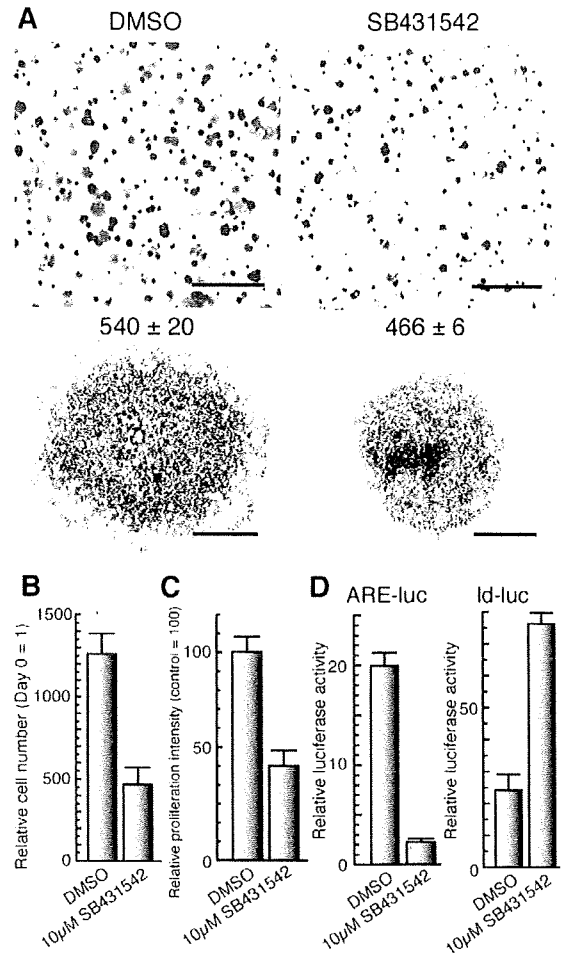


Fig. 2. SB-431542 inhibited ES cell propagation. (A) Colony morphologies of MGZ5 cells treated with SB-431542. MGZ5 cells were seeded at 2000 cells/well in six-well plates and cultured in FCS-containing medium supplemented with 10 μ M SB-431542 (right) or DMSO (as control, left) for 1 week. Numbers indicate numbers of colonies appearing ($n=3$). Each lower panel shows AP staining. Bars, 5 mm (upper panels); 200 μ m (lower panels). (B) Relative numbers of cells treated with SB-431542 or DMSO present on Day 7 of culture compared with that at Day 0. Each bar represents the mean ± s.e.m. ($n=3$). (C) Relative proliferation intensity is shown as total cell number/number of colonies appearing, compared with that of cells treated with DMSO (100%). Each bar represents the mean ± s.e.m. ($n=3$). (D) Luciferase reporter assay of MGZ5 cells transfected with reporter constructs (ARE-luc reporter or Id-1-luc reporter) and treated with SB-431542 or DMSO (as a control). Each bar represents mean ± s.e.m. ($n=3$).

showed that the elevated expression of *Smad7* reverted to normal in Smad7-10⁻ ES cells. We measured the growth ratios of fSmad7-10⁺, fSmad7-10⁻ and EB3 ES cells by determining cell numbers at 1, 3 and 5 days after seeding. Proliferation and plating efficiency of fSmad7-10⁺ ES cells was significantly decreased by expression of *Smad7* transgene, as found with the episomal expression system (Fig. 3C-E). However, upon removal of the *Smad7* transgene, proliferation of fSmad7-10⁻